RÉPUBLIQUE FRANÇAISE
Liberté
Égalité
Fraternité

SORBONNE UNIVERSITÉ
CRÉATEURS DE FUTURS DEPUIS 1257

LESIA l'Observatoire de Paris | PSL

Laboratoire d'Études Spatiales et d'Instrumentation en Astrophysique

cnes
CENTRE NATIONAL D'ÉTUDES SPATIALES

LsPRESSO : "Large scale Plasma Radio Emission Simulation of Spacecraft Observations",

Characterization of the Jovian Narrowband Kilometric Emission with Juno/Waves

---

Adam Boudouma
3rd year PhD student

PhD Supervisor : Philippe ZARKA (LESIA, PSL, Obs)
PhD Co-supervisor : Laurent LAMY (LESIA, LAM, Obs)
CNES supervisor : Kader ASMIF

Giant planets magnetosphere

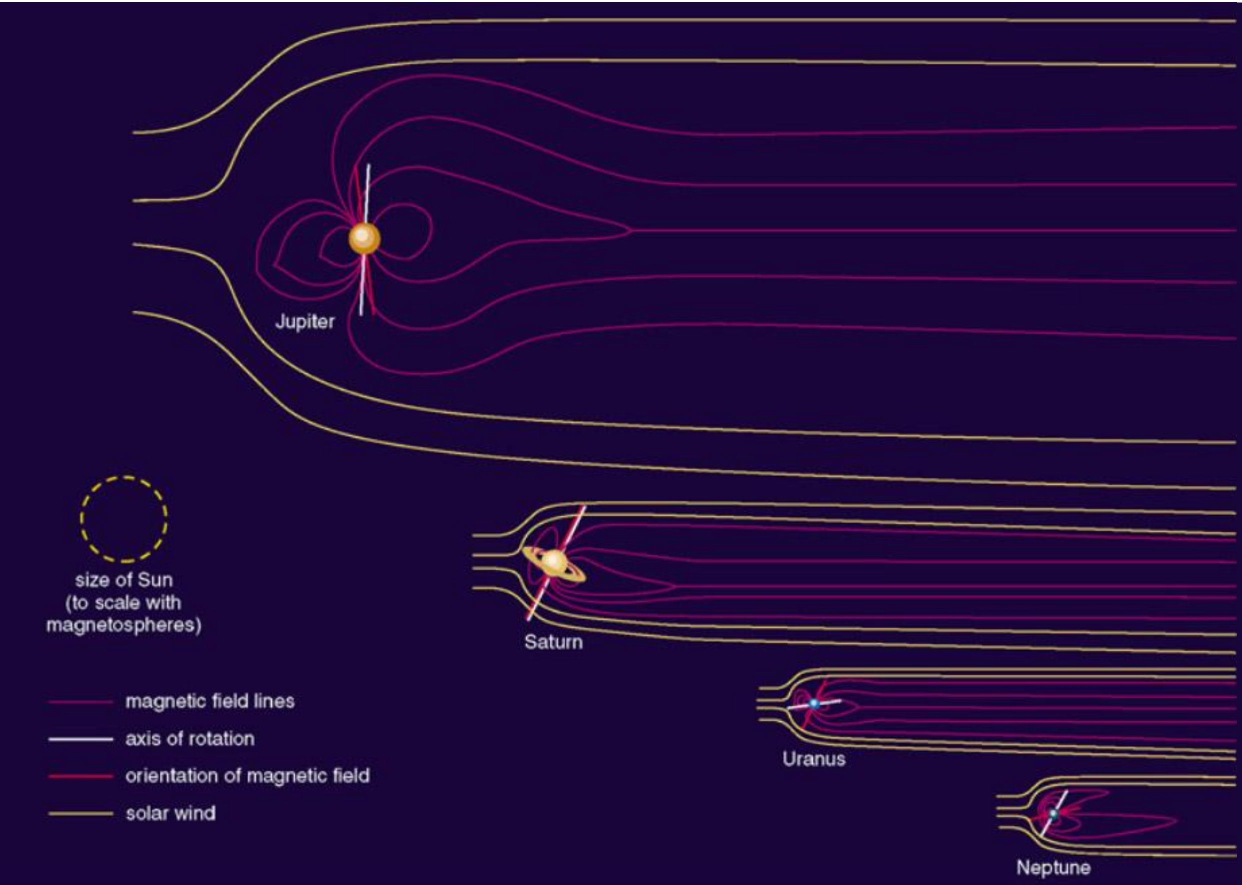

Jovian magnetosphere

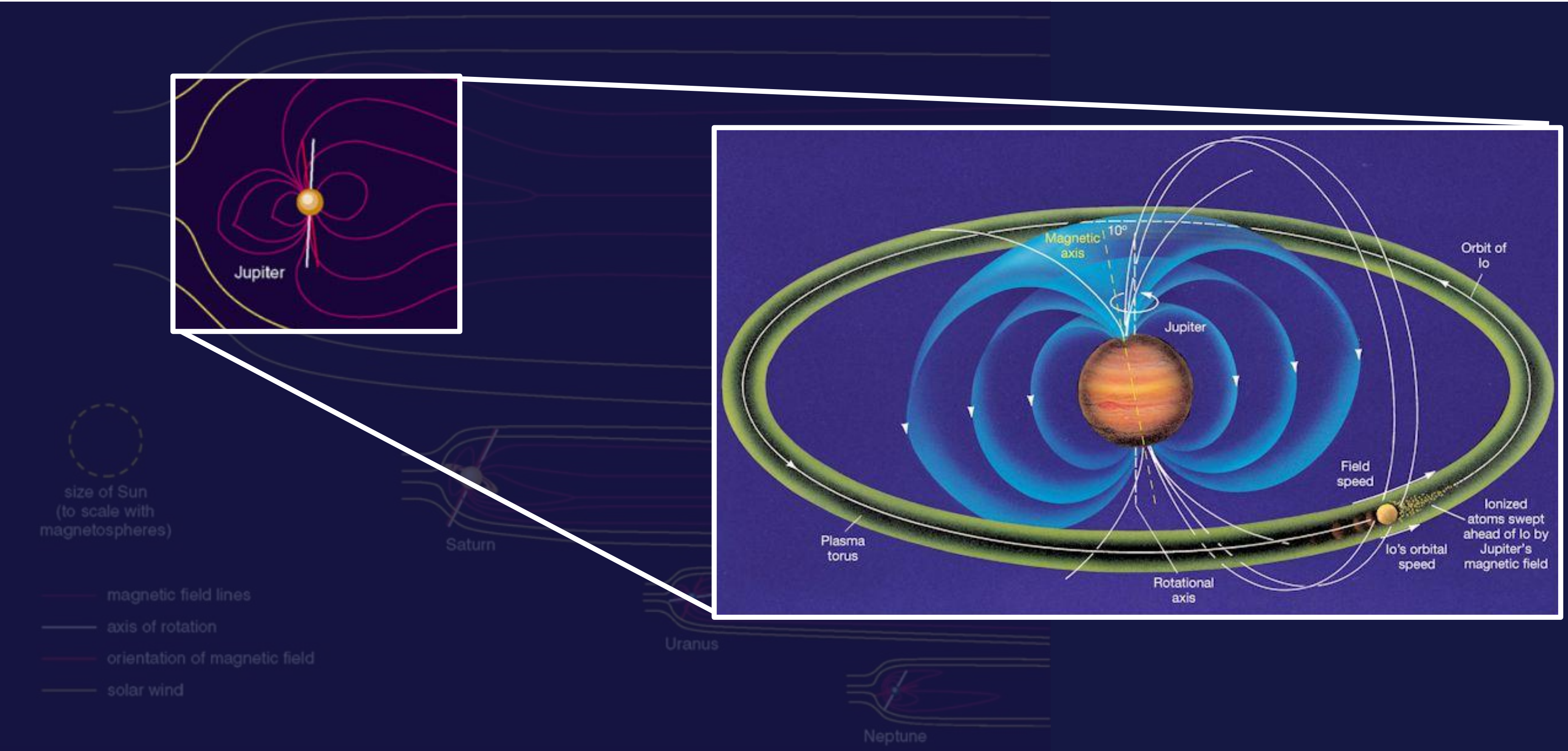

Jovian radio emissions

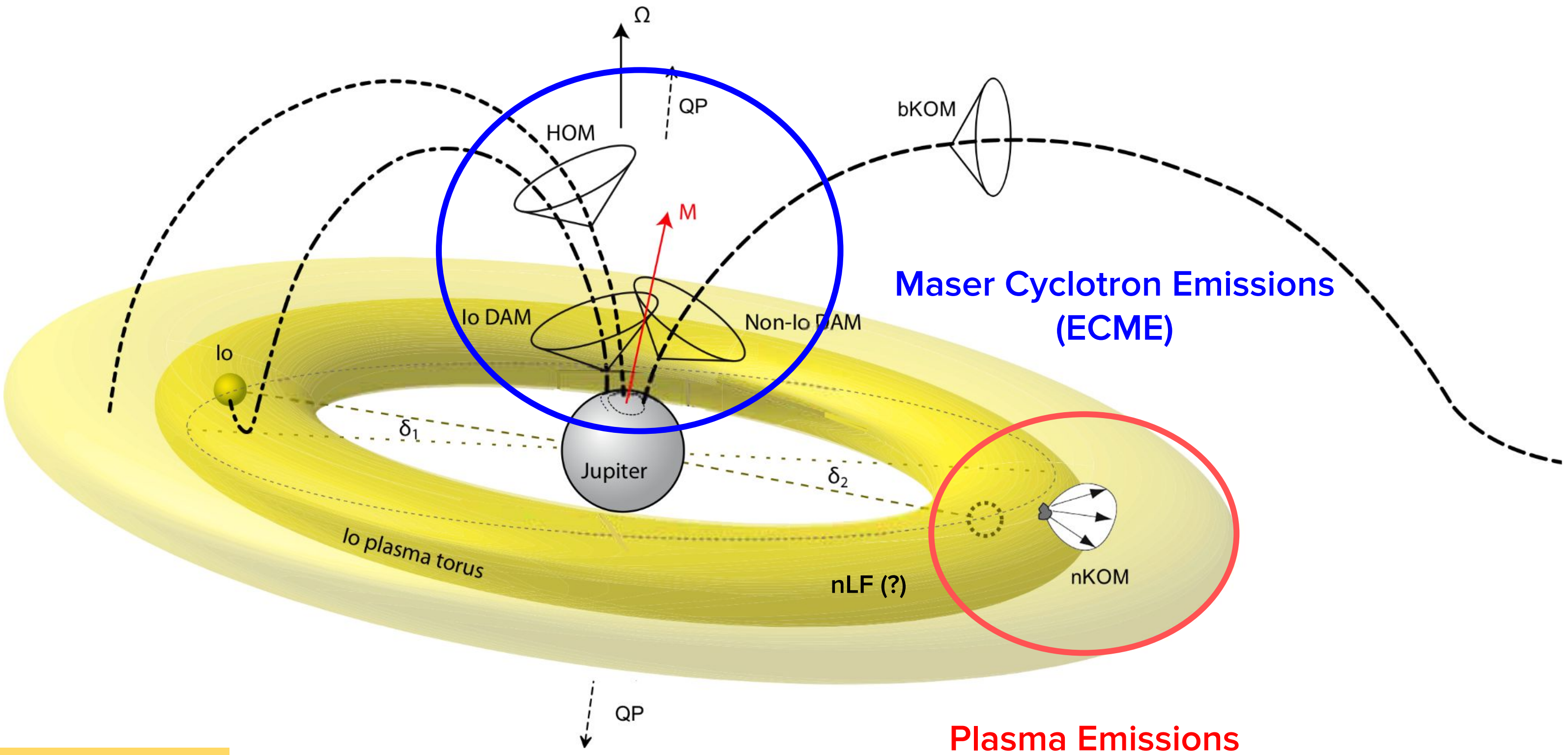

Zarka 2000

Jovian radio emissions

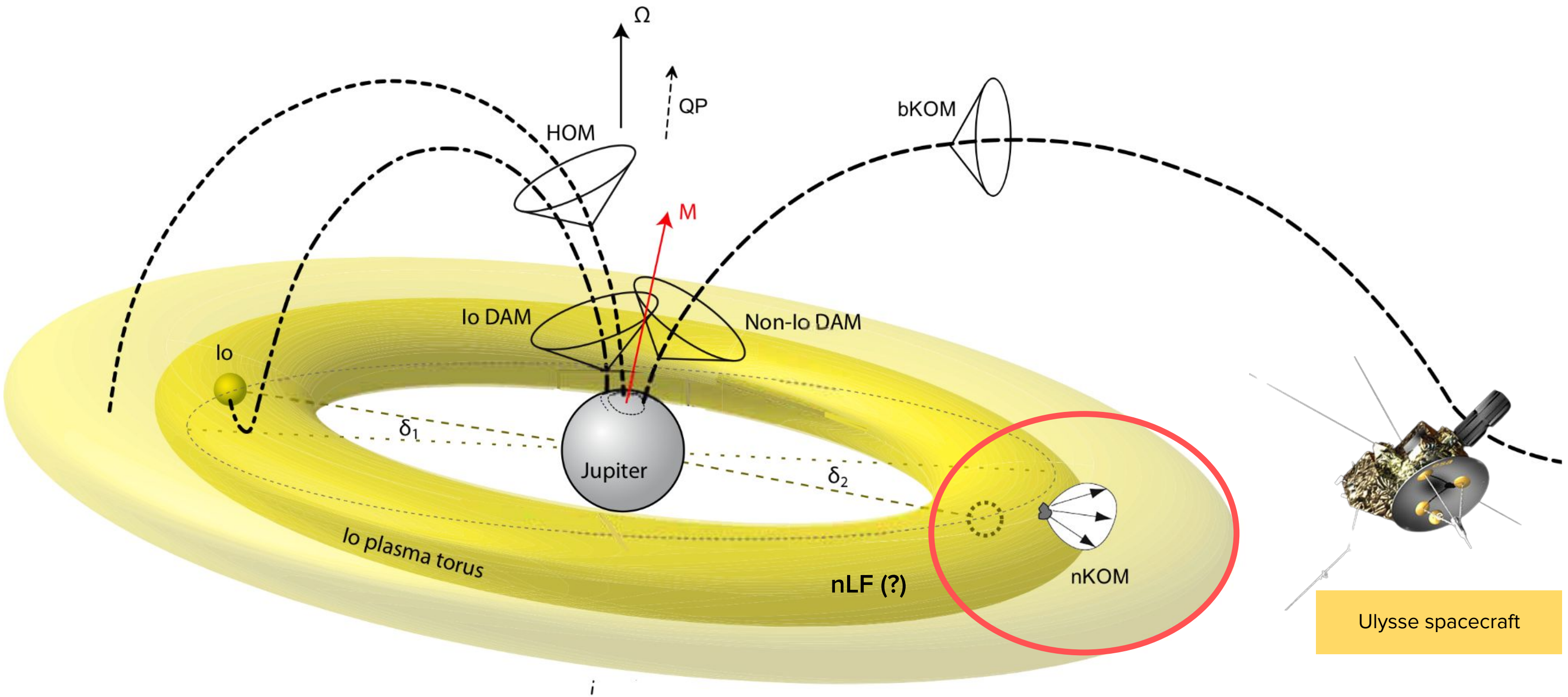

Zarka 2000

- **Ulysse** observation : **narrowband kilometric emissions (nKOM)**
- **nKOM** radiosources **located inside the Io plasma torus** (Reiner et al. 1993)
  - ↳ **nKOM = plasma emission**

Juno Spacecraft

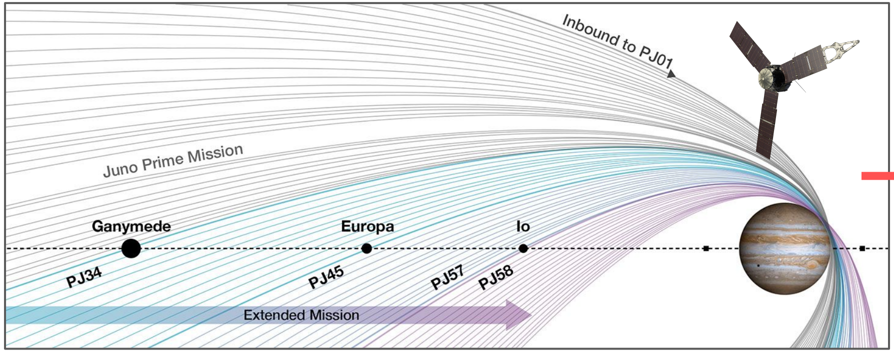

Juno's trajectory for :
"Juno Prime Mission" : 2016-2023
"Juno Extended Mission" : 2024 - 2026

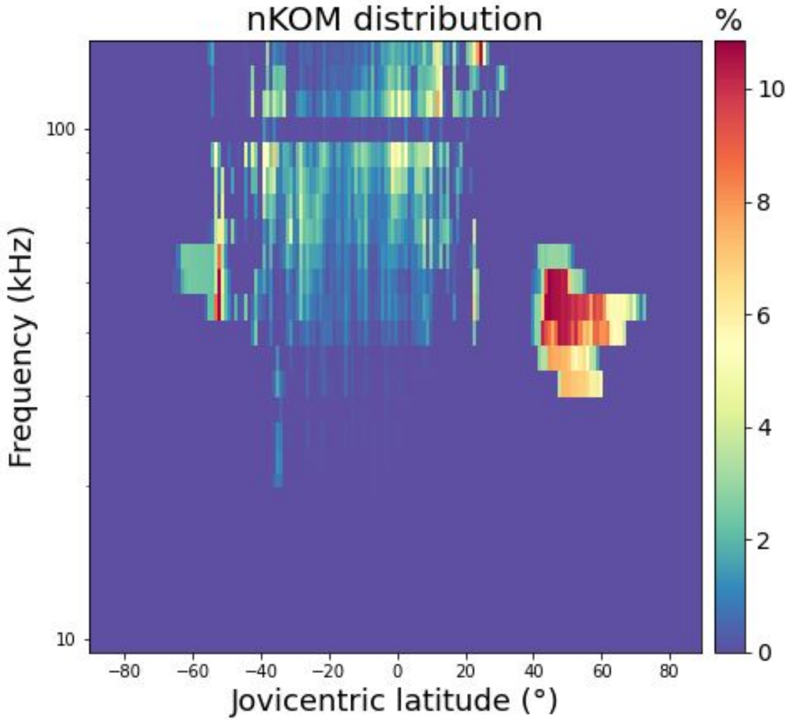

Occurrence vs. latitude & frequency distribution (in %) of the nKOM for the Juno/Waves 2016-2019 observations (Louis et al. 2021)

LsPRESSO - Localize & constraint plasma radio emission

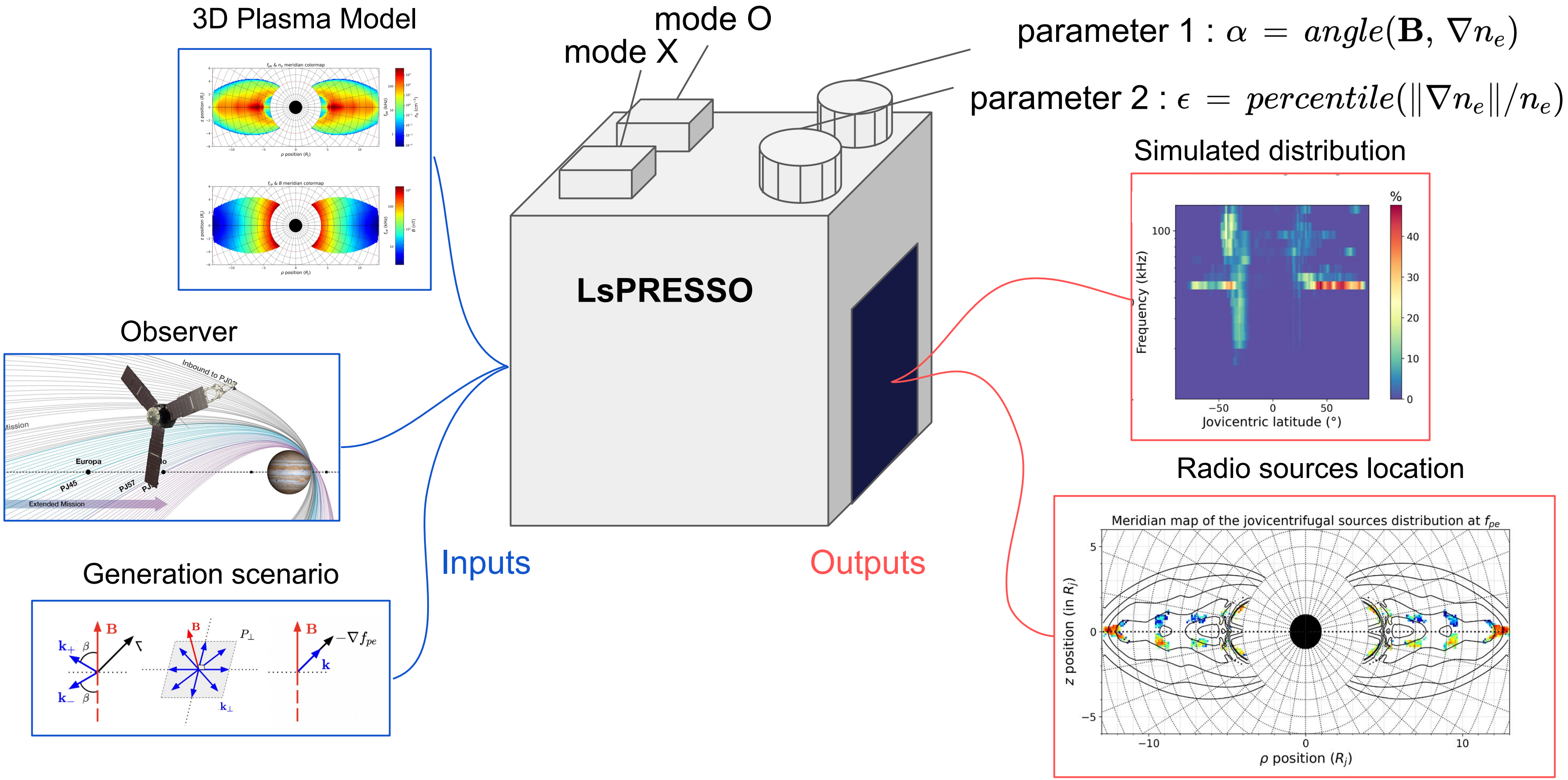

Simulation Setup

3D Plasma model:

- **Electron density**: Imai's 2016 diffusive density model
- **Magnetic field**: VIP4 (Connerney et al. 1998)

Observer:

- Juno's **2016-2019 trajectory** (Louis et al. 2021)
- Waves antenna from **1 kHz to 141 kHz**

Assumptions:

- Emission **straight line propagation**
- **Full-absorption** above the cutoff-frequency either **O- or X-mode**
- **Time averaged** emission occurrence

Limitations:

- Electron density modeled **limited to 4-13 Rj**
- Electron density **cylindrical symmetry**
- **Large meshgrid** (dx = 0.1 Rj ~ 7000 km)

nKOM Generation Parameters & Scenarios

- nKOM are expected to be produced **in ordinary (O-) or extraordinary (X-) mode** by **conversion mode mechanisms**
- **In a cold collisionless magnetized plasma**, conversion mode mechanisms efficiency are controlled by **2 parameters:**
  - $angle(\mathbf{B},\, \nabla n_e)$
  - $\|\nabla n_e\|/n_e$
- **At large scale**, we have established **3 scenario** that can describe the nKOM:

Scenario 1 : Jones 1987 theory constraints

Emission frequency : f_{pe}

Emission beaming :

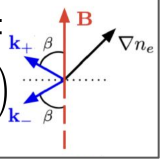

$\beta = \arctan\left(\sqrt{fpe/fce}\right)$

Scenario 2 : Fung & Papadopoulos 1987 theory constraints

Emission frequency : $2\,f_{uh}$

Emission beaming :

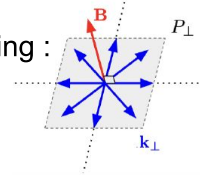

Scenario 3 : Gradient directed fpe emissions

Emission frequency : f_{pe}

Emission beaming :

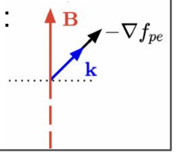

Plasma frequency : $f_{pe} = f(n_e)$

Electron cyclotron frequency : $f_{ce} = f(B)$

Upper Hybrid frequency : $f_{uh} = \sqrt{(f_{pe})^2 + (f_{ce})^2}$

nKOM Generation Parameters & Scenarios

- nKOM are expected to be produced **in ordinary (O-) or extraordinary (X-) mode** by **conversion mode mechanisms**
- **In a cold collisionless magnetized plasma**, conversion mode mechanisms efficiency are controlled by **2 parameters:**
  - $angle(\mathbf{B}, \nabla n_e)$
  - $\|\nabla n_e\|/n_e$
- **At large scale**, we have established **3 scenario** that can describe the nKOM:

Scenario 1 : Jones 1987 theory constraints

Emission frequency : f_{pe}

Emission beaming :

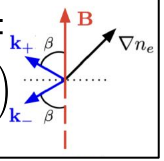

$\beta = \arctan\left(\sqrt{fpe/fce}\right)$

Scenario 2 : Fung & Papadopoulos 1987 theory constraints

Emission frequency : $2f_{uh}$

Emission beaming :

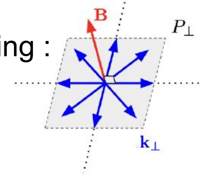

Scenario 3 : Gradient directed fpe emissions

Emission frequency : f_{pe}

Emission beaming :

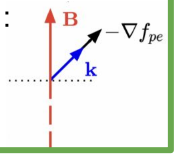

Plasma frequency : $f_{pe} = f(n_e)$

Electron cyclotron frequency : $f_{ce} = f(B)$

Upper Hybrid frequency : $f_{uh} = \sqrt{(f_{pe})^2 + (f_{ce})^2}$

only scenario #3 results match the nKOM observations

Scenario #3 Results **O-mode** : Distributions and Sources Location

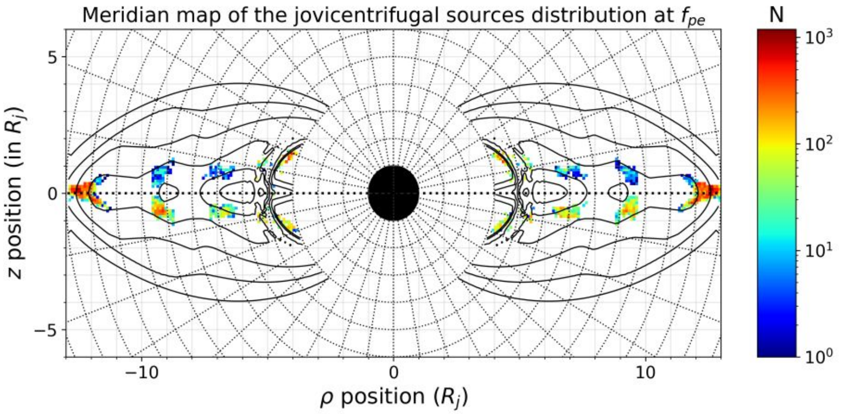

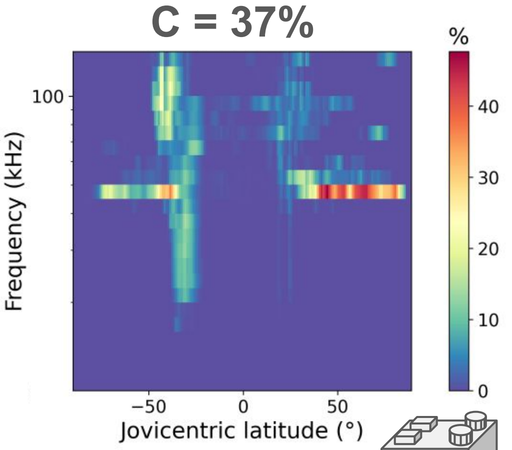

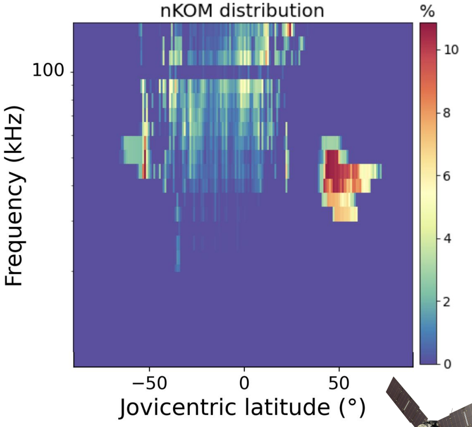

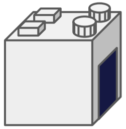

Scenario #3 O-mode result with the highest correlation coefficient. Panel (a) is the correlation-inclusion coefficient evolution, (b) the distribution obtained from the distribution with *p* > 85% of max(C*) and (c) the corresponding sources locations in the plasma. The contours on panel (c) correspond to the plasma frequency contours at 10, 20, 40, 80, 160 and 320 kHz

Scenario #3 Results **O-mode** : Distributions and Sources Location

Compatible with the observations !

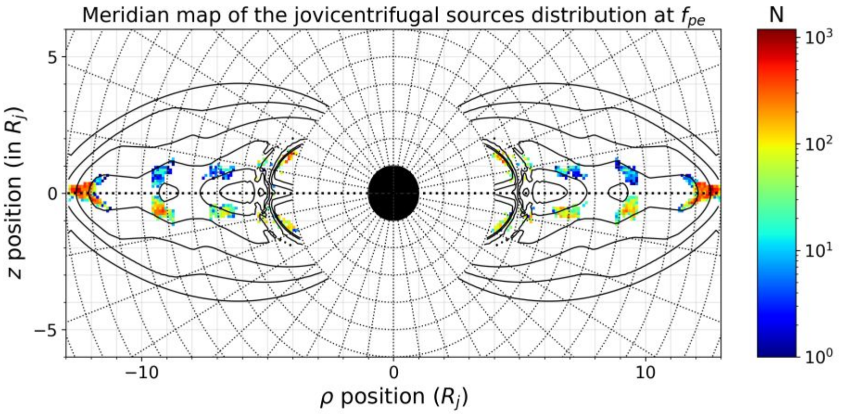

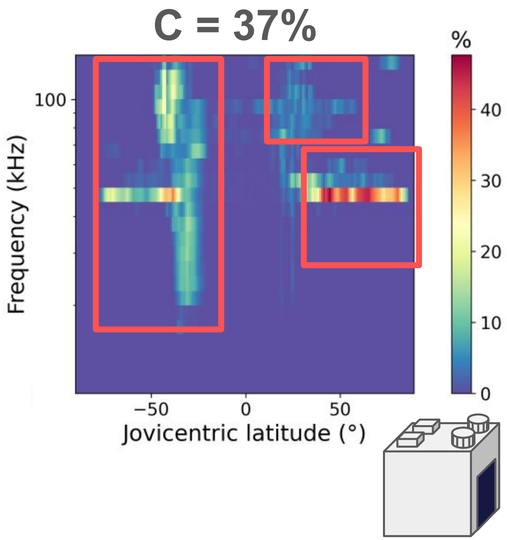

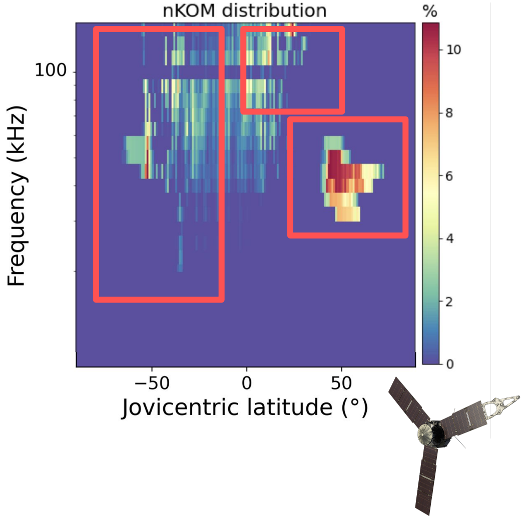

Scenario #3 O-mode result with the highest correlation coefficient. Panel (a) is the correlation-inclusion coefficient evolution, (b) the distribution obtained from the distribution with p > 85% of max(C*) and (c) the corresponding sources locations in the plasma. The contours on panel (c) correspond to the plasma frequency contours at 10, 20, 40, 80, 160 and 320 kHz

Scenario #3 Results **O-mode** : Distributions and Sources Location

Radio sources near the jovicentrifugal equator !

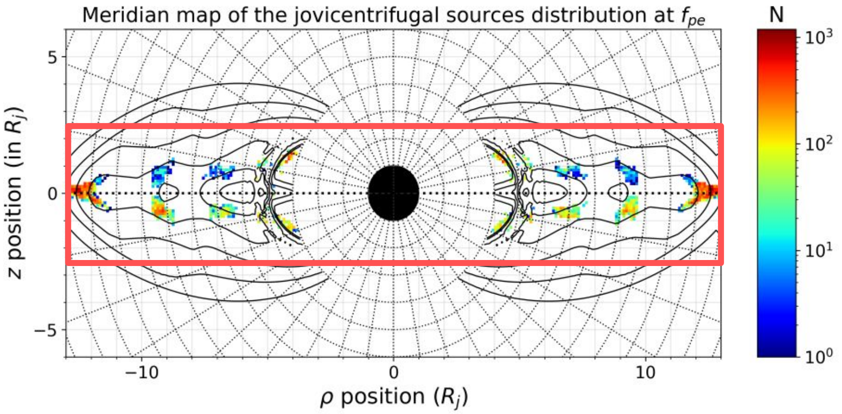

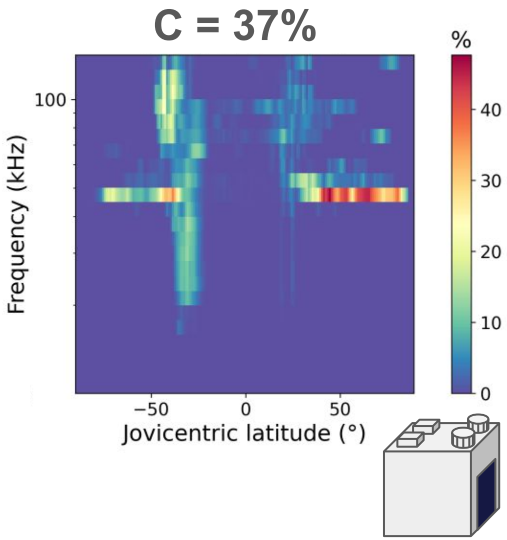

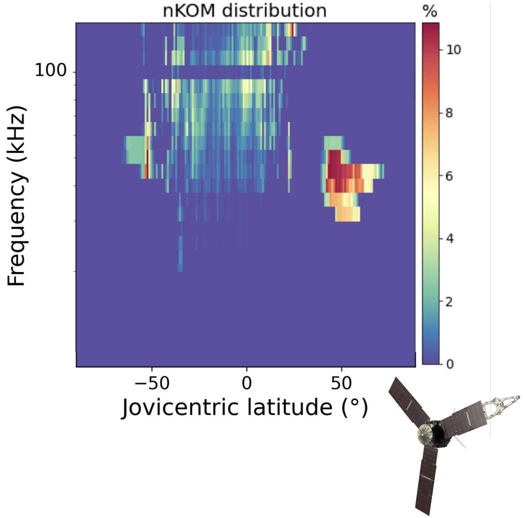

Scenario #3 O-mode result with the highest correlation coefficient. Panel (a) is the correlation-inclusion coefficient evolution, (b) the distribution obtained from the distribution with *p* > 85% of max(C*) and (c) the corresponding sources locations in the plasma. The contours on panel (c) correspond to the plasma frequency contours at 10, 20, 40, 80, 160 and 320 kHz

Scenario #3 Results **O-mode** : Distributions and Sources Location

Located in the inner-edge of the plasma torus

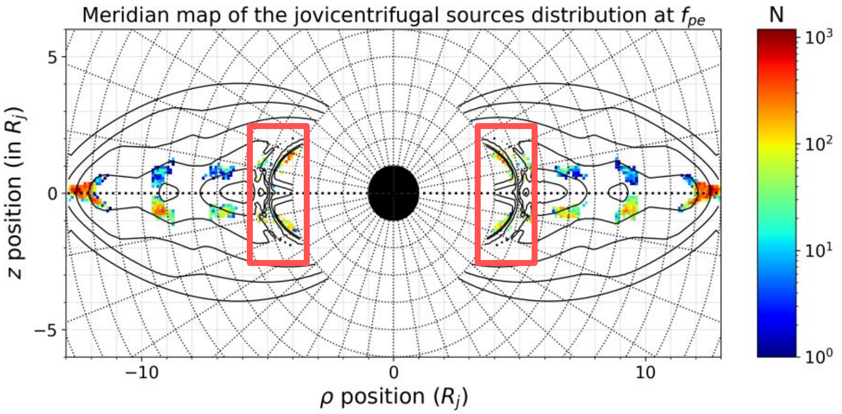

C = 37%

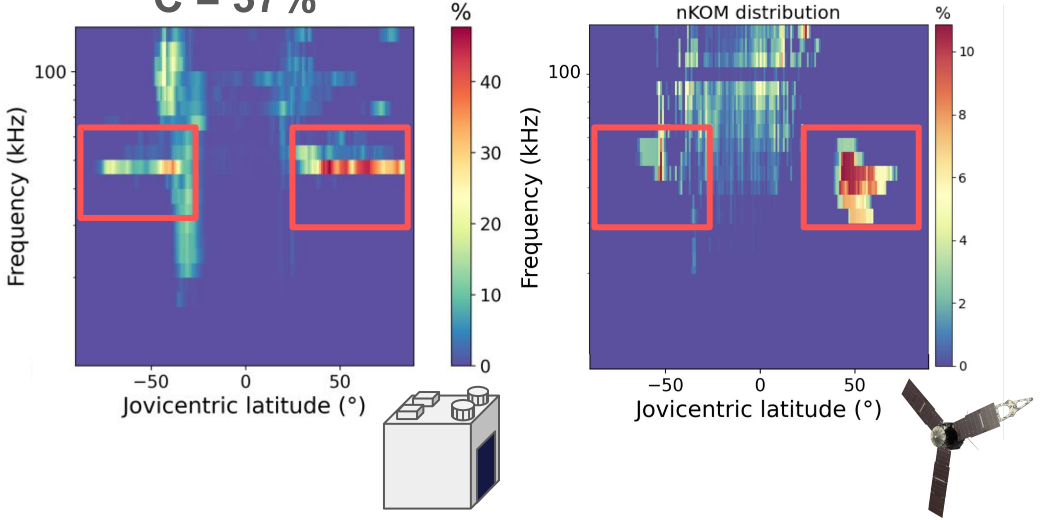

Scenario #3 O-mode result with the highest correlation coefficient. Panel (a) is the correlation-inclusion coefficient evolution, (b) the distribution obtained from the distribution with p > 85% of max(C*) and (c) the corresponding sources locations in the plasma. The contours on panel (c) correspond to the plasma frequency contours at 10, 20, 40, 80, 160 and 320 kHz

Scenario #3 Results **O-mode** : Distributions and Sources Location

Located from the outer-edge to the inner part of the plasma torus

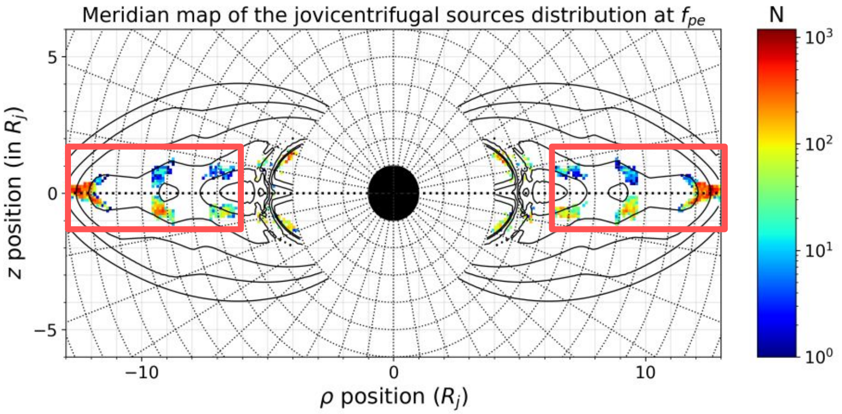

C = 37%

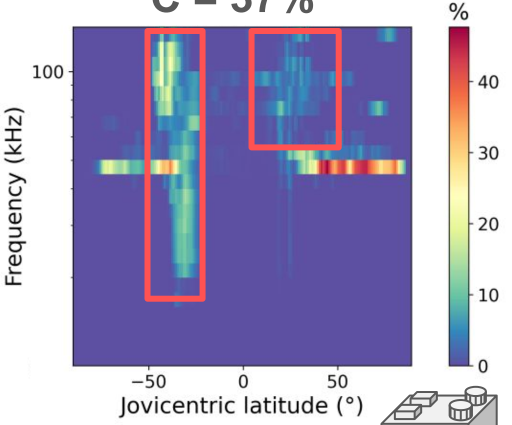

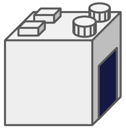

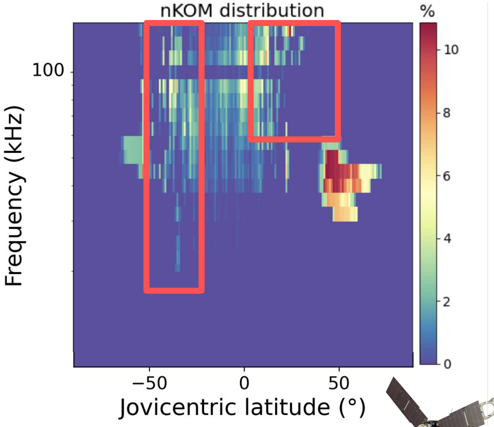

Scenario #3 O-mode result with the highest correlation coefficient. Panel (a) is the correlation-inclusion coefficient evolution, (b) the distribution obtained from the distribution with *p* > 85% of max(C*) and (c) the corresponding sources locations in the plasma. The contours on panel (c) correspond to the plasma frequency contours at 10, 20, 40, 80, 160 and 320 kHz

Scenario #3 Results **O-mode** : Distributions and Sources Location

No occurrences ?
Incomplete prediction

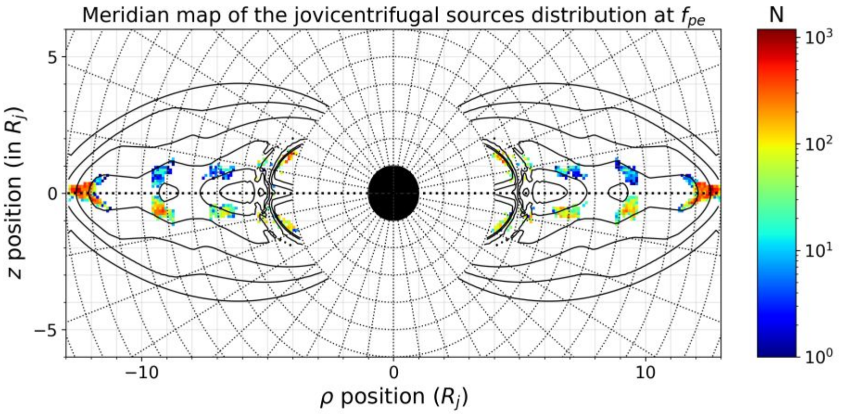

C = 37%

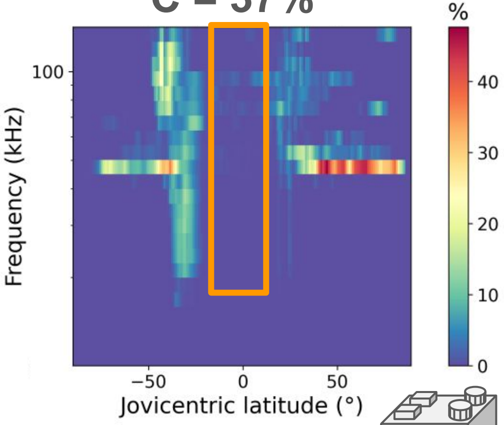

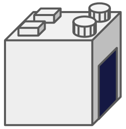

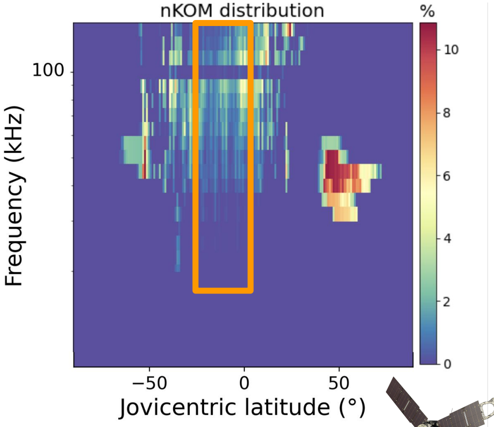

Scenario #3 O-mode result with the highest correlation coefficient. Panel (a) is the correlation-inclusion coefficient evolution, (b) the distribution obtained from the distribution with $p > 85\%$ of max(C*) and (c) the corresponding sources locations in the plasma. The contours on panel (c) correspond to the plasma frequency contours at 10, 20, 40, 80, 160 and 320 kHz

Scenario #3 Results **X-mode** : Distributions and Sources Location

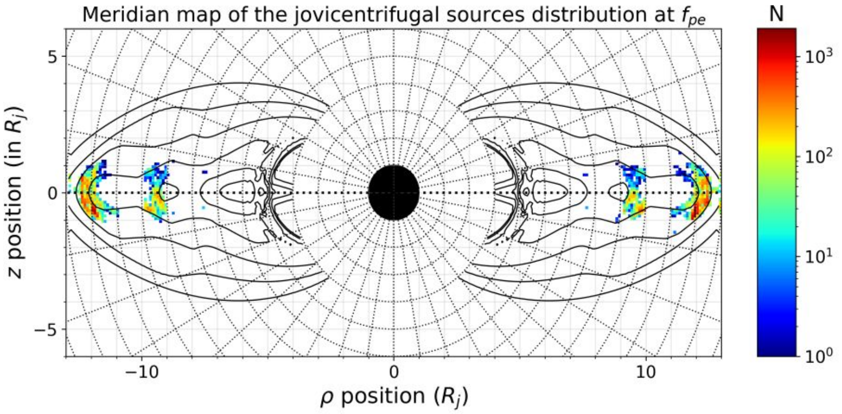

C = 22%

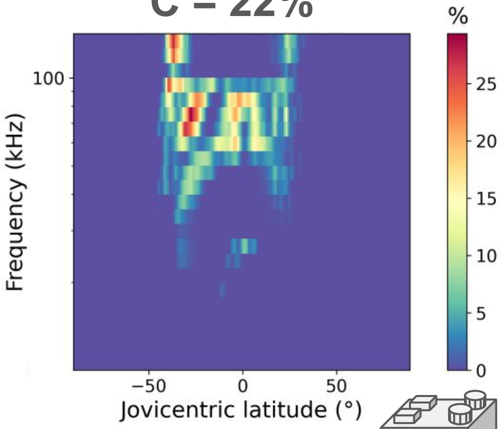

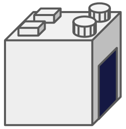

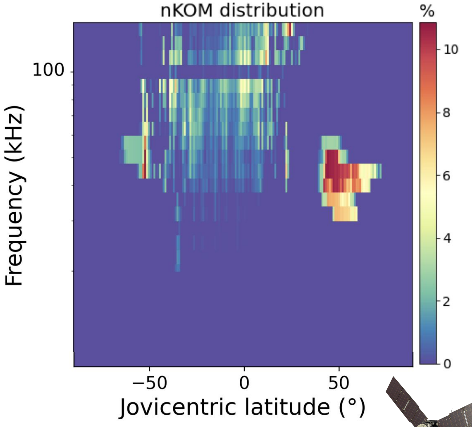

Scenario #3 O-mode result with the highest correlation coefficient. Panel (a) is the correlation-inclusion coefficient evolution, (b) the distribution obtained from the distribution with *p* > 85% of max(C*) and (c) the corresponding sources locations in the plasma. The contours on panel (c) correspond to the plasma frequency contours at 10, 20, 40, 80, 160 and 320 kHz

Scenario #3 Results **X-mode** : Distributions and Sources Location

Compatible with the observations !

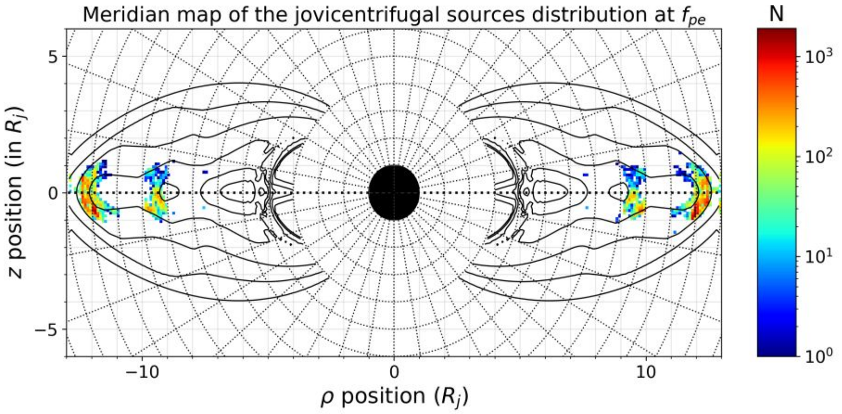

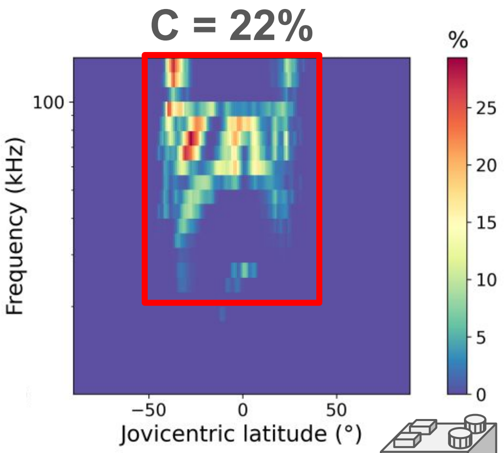

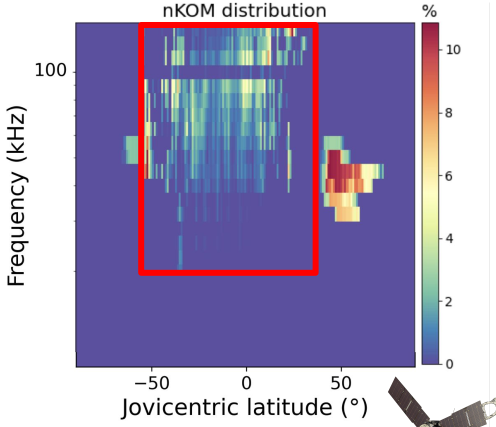

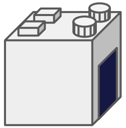

Scenario #3 O-mode result with the highest correlation coefficient. Panel (a) is the correlation-inclusion coefficient evolution, (b) the distribution obtained from the distribution with *p* > 85% of max(C*) and (c) the corresponding sources locations in the plasma. The contours on panel (c) correspond to the plasma frequency contours at 10, 20, 40, 80, 160 and 320 kHz

Scenario #3 Results **X-mode** : Distributions and Sources Location

Located from the outer-edge to the middle part of the plasma torus

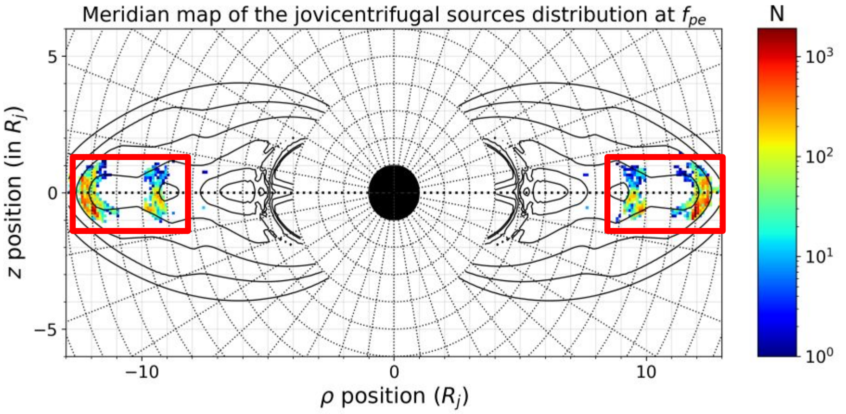

Scenario #3 O-mode result with the highest correlation coefficient. Panel (a) is the correlation-inclusion coefficient evolution, (b) the distribution obtained from the distribution with $p > 85\%$ of max(C*) and (c) the corresponding sources locations in the plasma. The contours on panel (c) correspond to the plasma frequency contours at 10, 20, 40, 80, 160 and 320 kHz

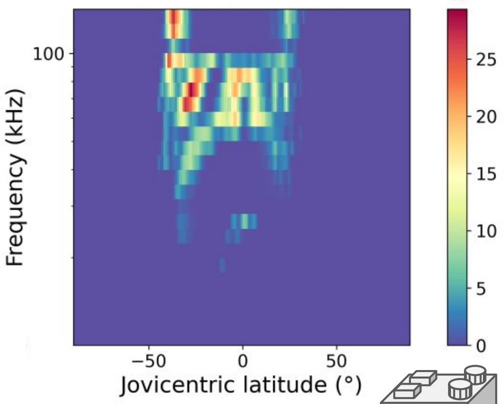

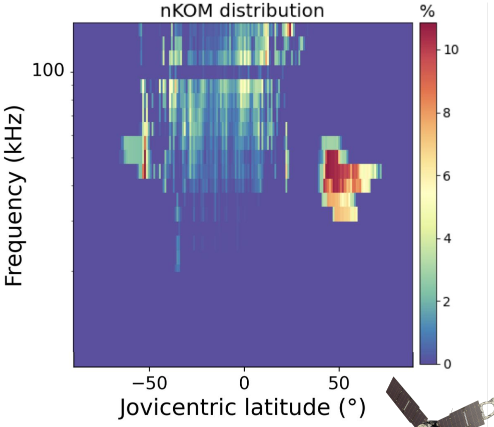

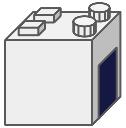

Scenario #3 Results **X-mode** : Distributions and Sources Location

No occurrences ?
Incomplete prediction

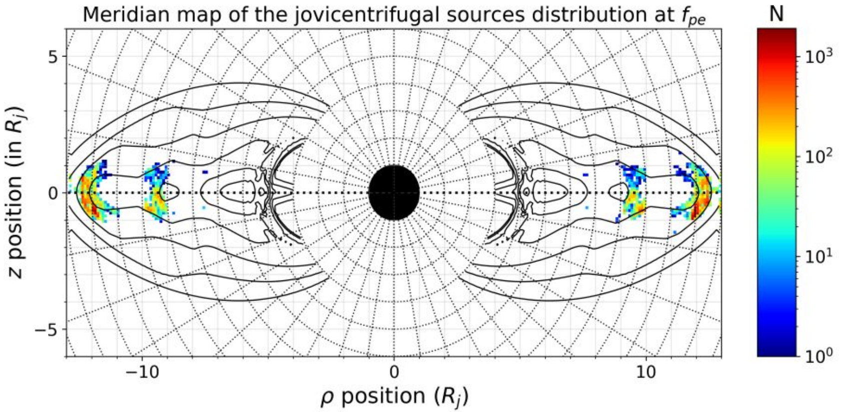

C = 22%

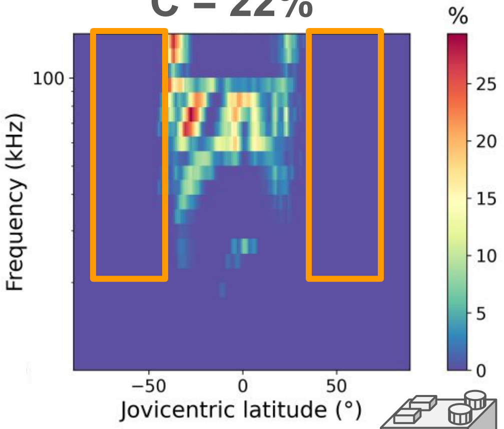

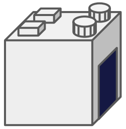

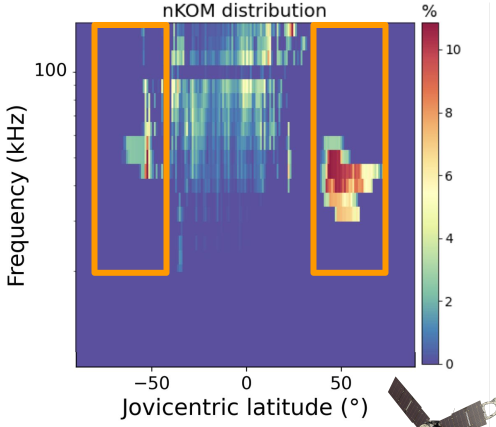

Scenario #3 O-mode result with the highest correlation coefficient. Panel (a) is the correlation-inclusion coefficient evolution, (b) the distribution obtained from the distribution with p > 85% of max(C*) and (c) the corresponding sources locations in the plasma. The contours on panel (c) correspond to the plasma frequency contours at 10, 20, 40, 80, 160 and 320 kHz

Scenario #3 Results **X-mode** : Distributions and Sources Location

Seems complementary with O-mode simulation !

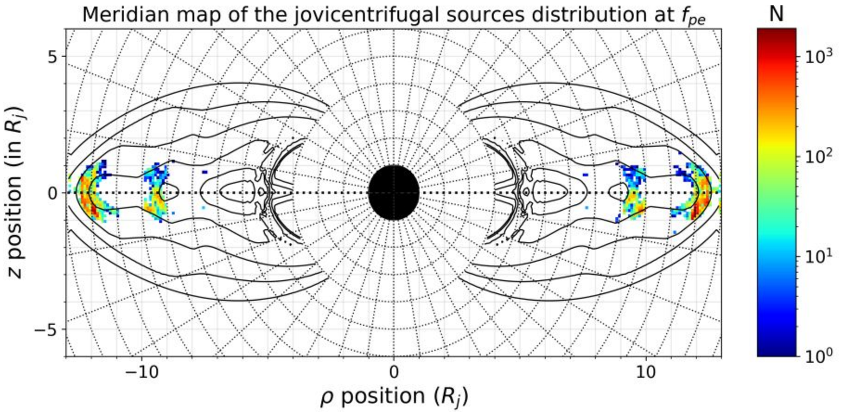

Scenario #3 O-mode result with the highest correlation coefficient. Panel (a) is the correlation-inclusion coefficient evolution, (b) the distribution obtained from the distribution with p > 85% of max(C*) and (c) the corresponding sources locations in the plasma. The contours on panel (c) correspond to the plasma frequency contours at 10, 20, 40, 80, 160 and 320 kHz

C = 22%

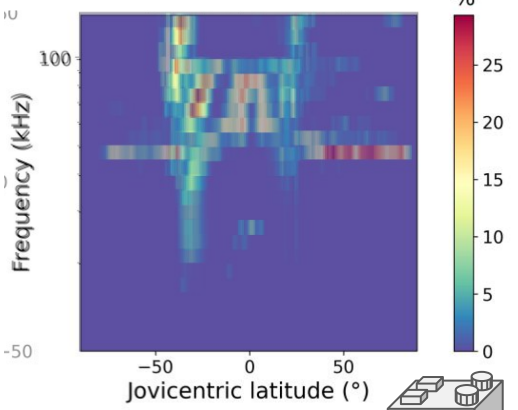

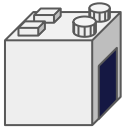

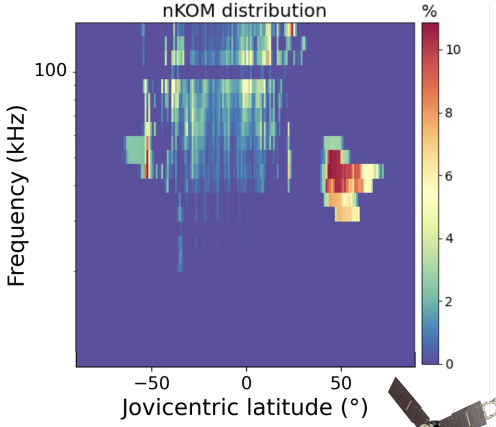

Merged Scenario #3 O- and X-modes simulations

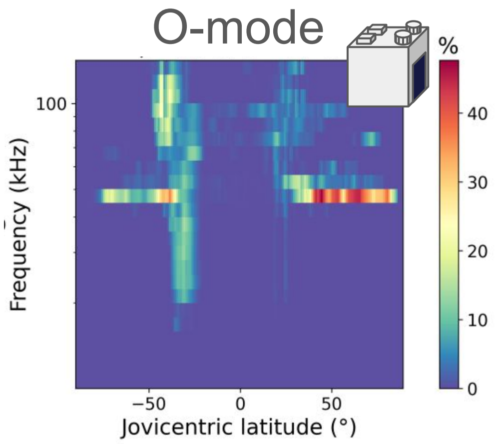

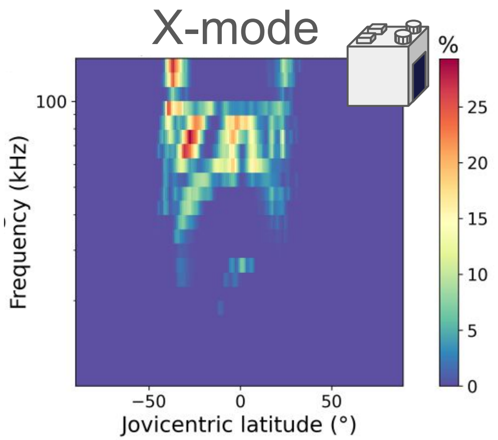

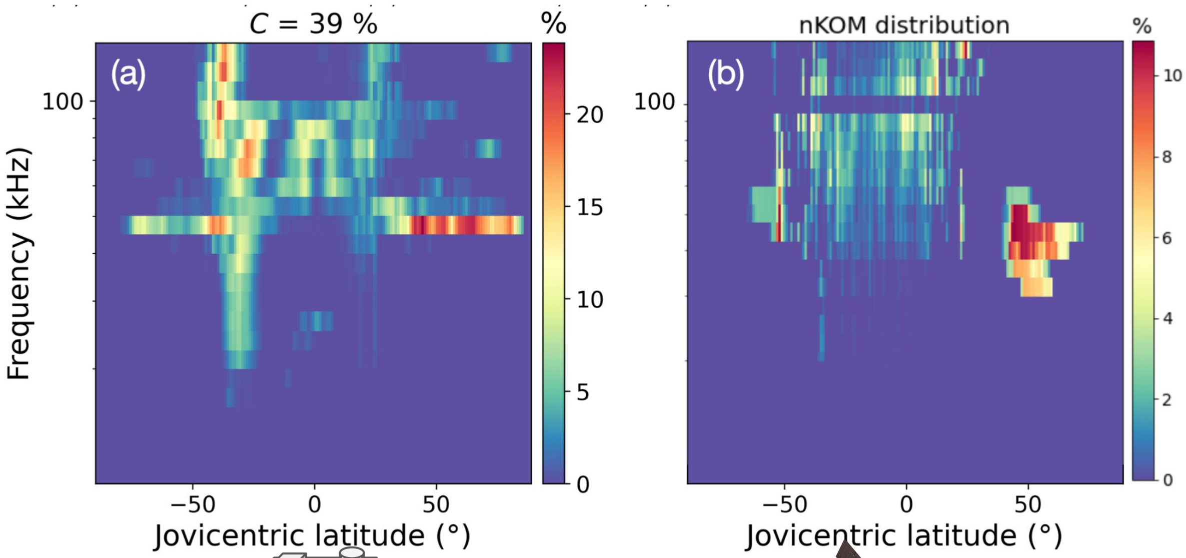

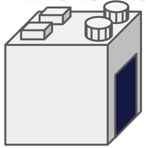

nKOM observations seems compatible with both O- and X-modes !

Merged Scenario #3 O- and X-modes simulations

O-mode

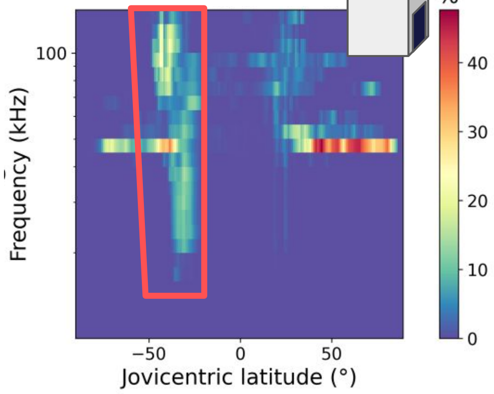

X-mode

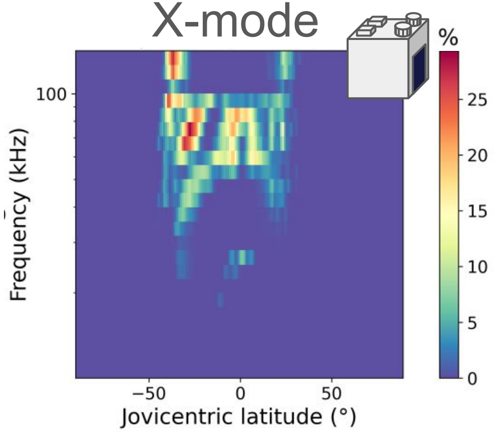

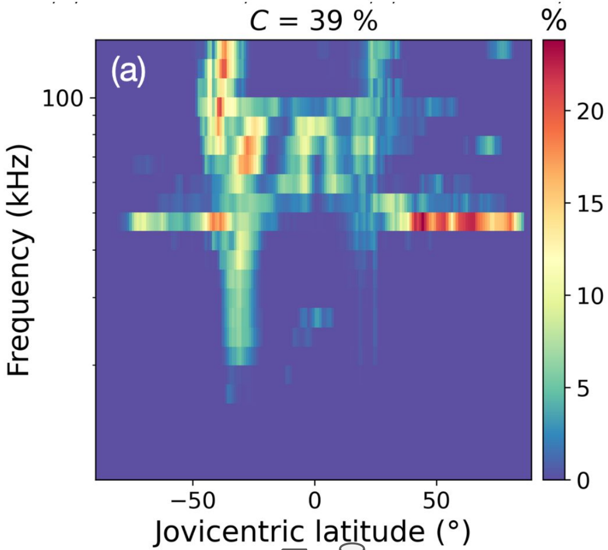

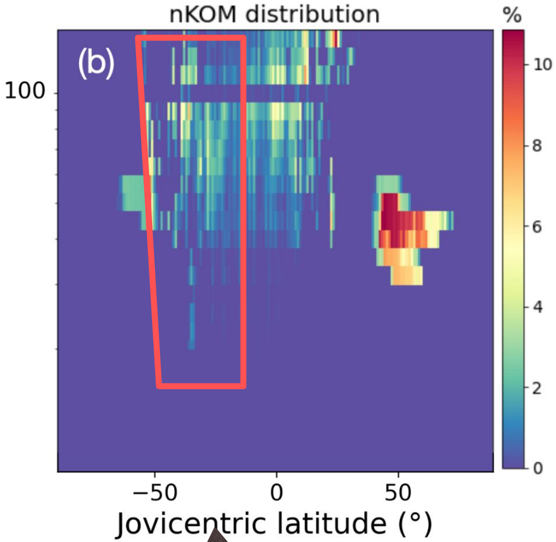

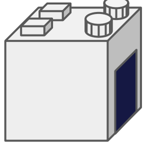

nKOM observations seems compatible with both O- and X-modes !

Merged Scenario #3 O- and X-modes simulations

O-mode

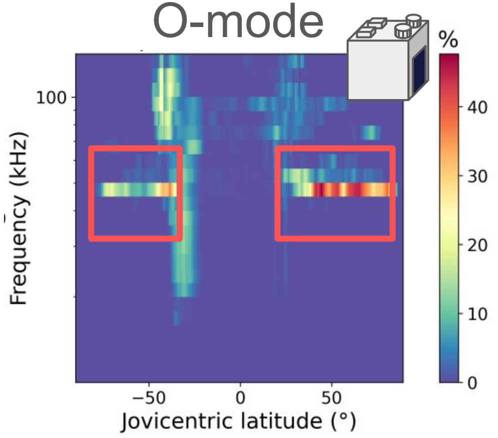

X-mode

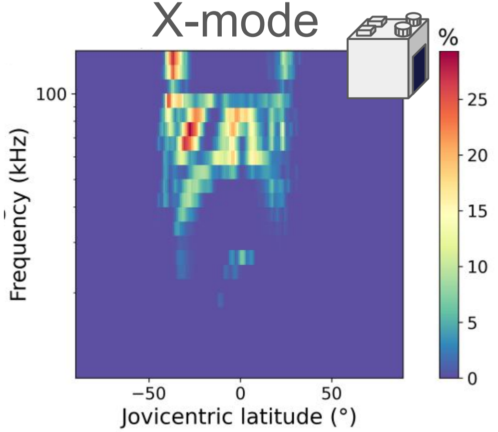

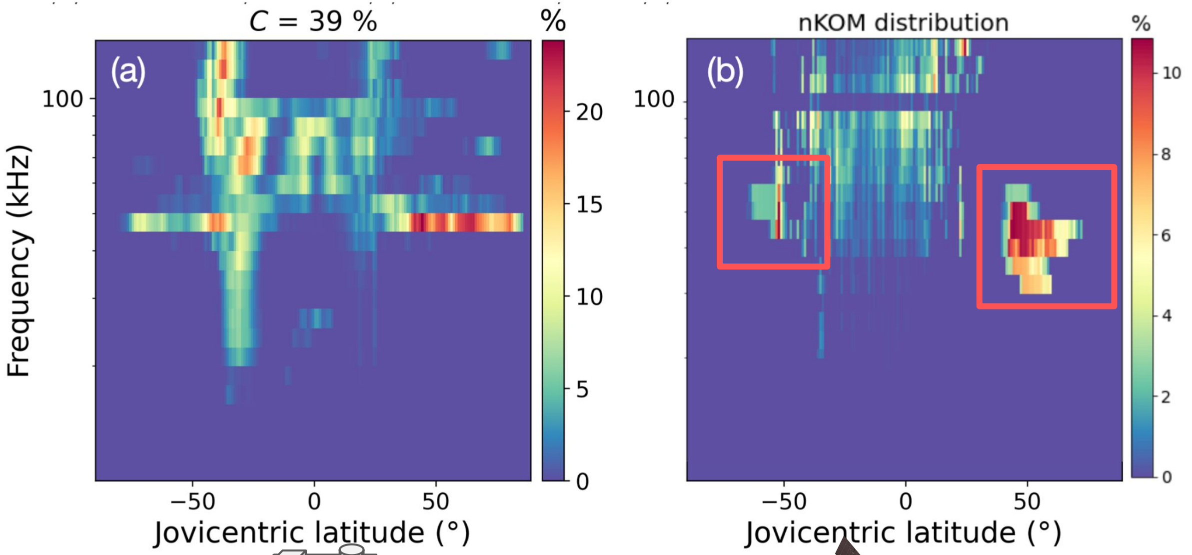

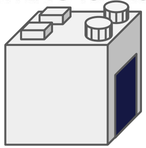

nKOM observations seems compatible with both O- and X-modes !

Merged Scenario #3 O- and X-modes simulations

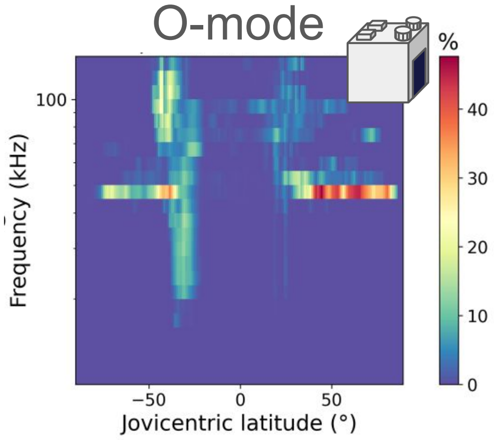

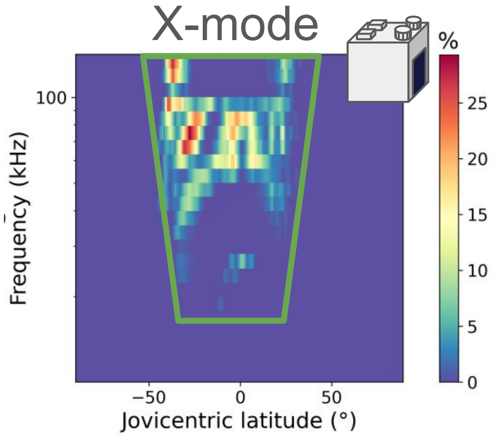

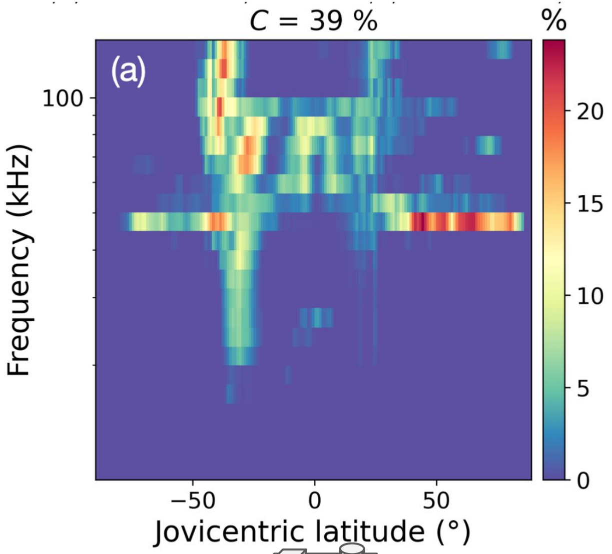

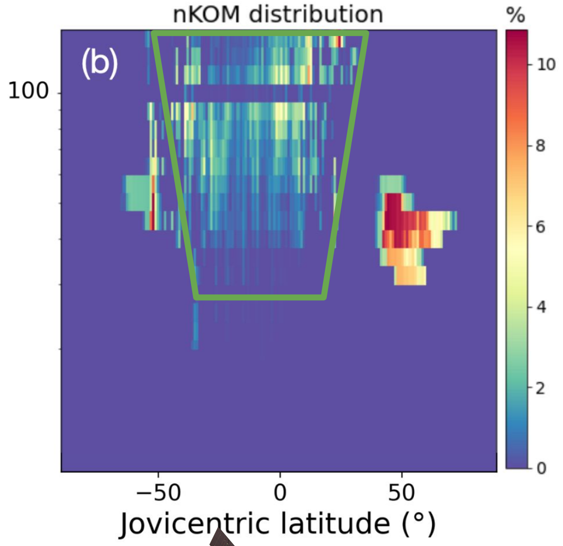

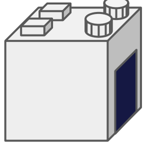

nKOM observations seems compatible with both O- and X-modes !

Summary

- **nKOM frequency** compatible with **emission generated at fpe**
- **nKOM beaming** compatible with emission **beaming along the frequency gradient** in the direction of the decreasing frequencies
- **nKOM observed** by Juno/Waves compatible with emission in **O-mode at high latitudes** and **X-mode at low latitudes**
- **nKOM radio sources** are distributed near the **jovicentrifugal equator** from the **inner-edge to the outer-edge** of the plasma torus

Juno/Waves Observations

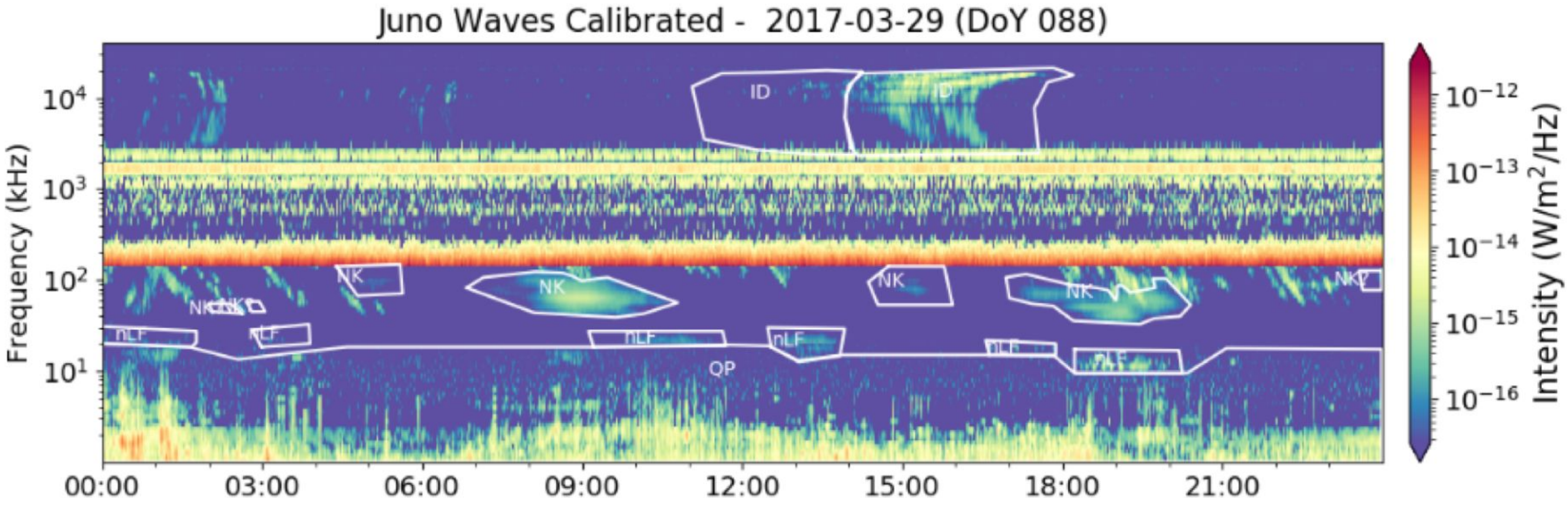

24h Calibrated dynamic spectra of the Juno/Waves observations (Louis et al. 2021)

Juno/Waves nKOM Observations

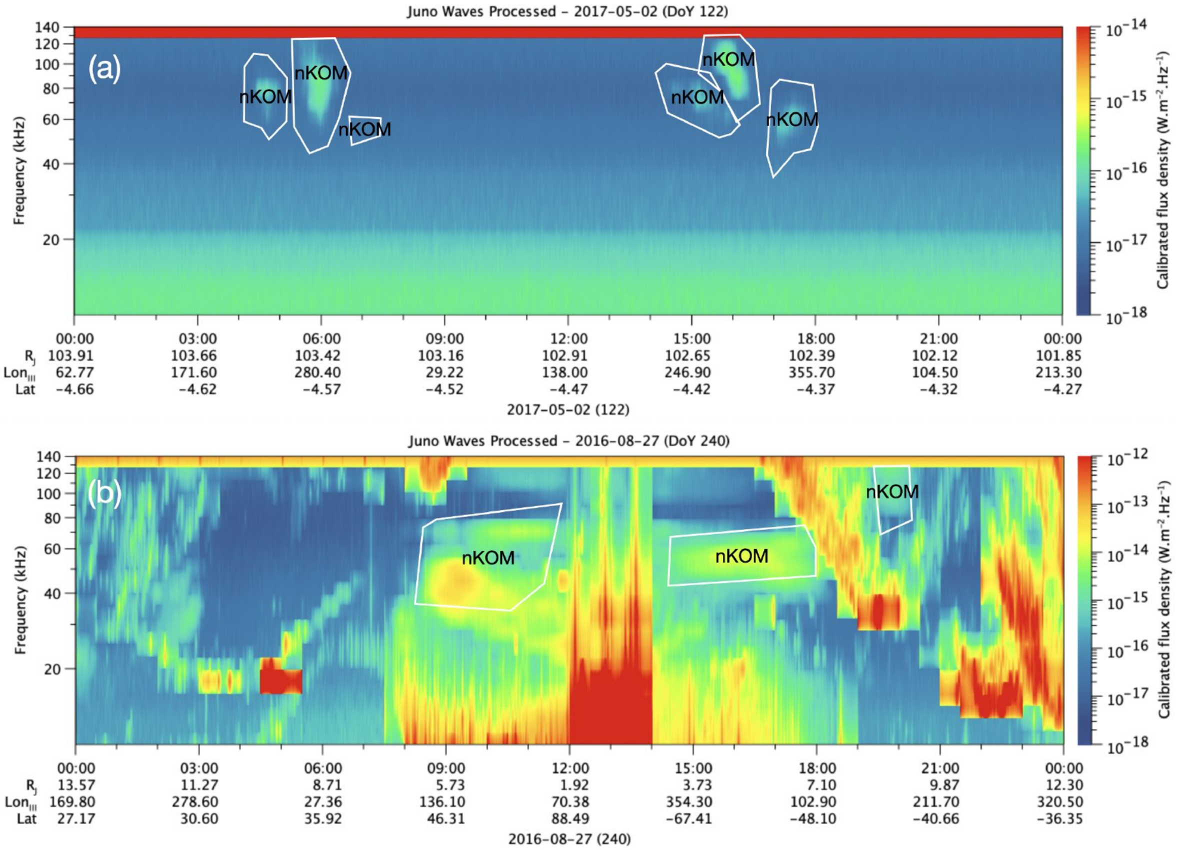

Low-Latitudes
High Radial Distances

24h Calibrated dynamic spectrum of the Juno/Waves observations of the nKOM

High-Latitudes
Low Radial Distances

Mode Conversion in the Magnetosphere

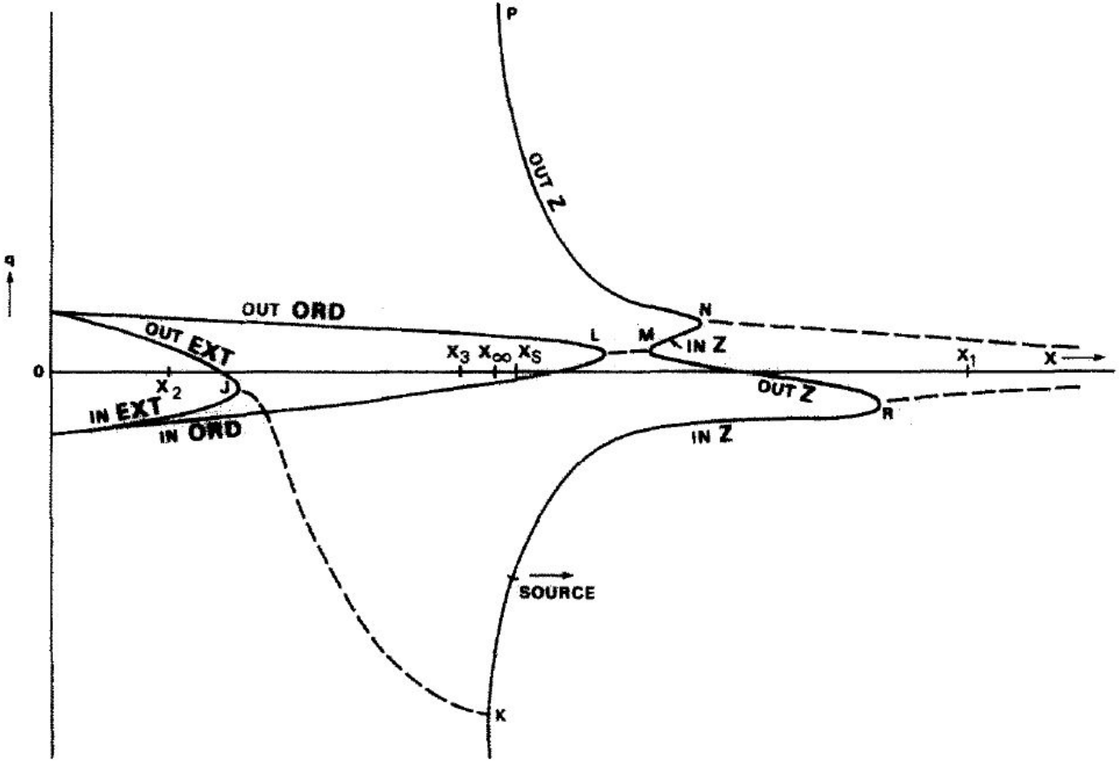

Fig. 1. Sketch, not to scale, showing how q depends on X when electron collisions are neglected and $Y < 1$. For the continuous curves q is real. The broken curves show $\mathrm{Re}(q)$ where two values of q are complex conjugates. The level where $X = 1$ is between L and M.

Emission Propagation in a Cold Magnetized Collisonless Plasma

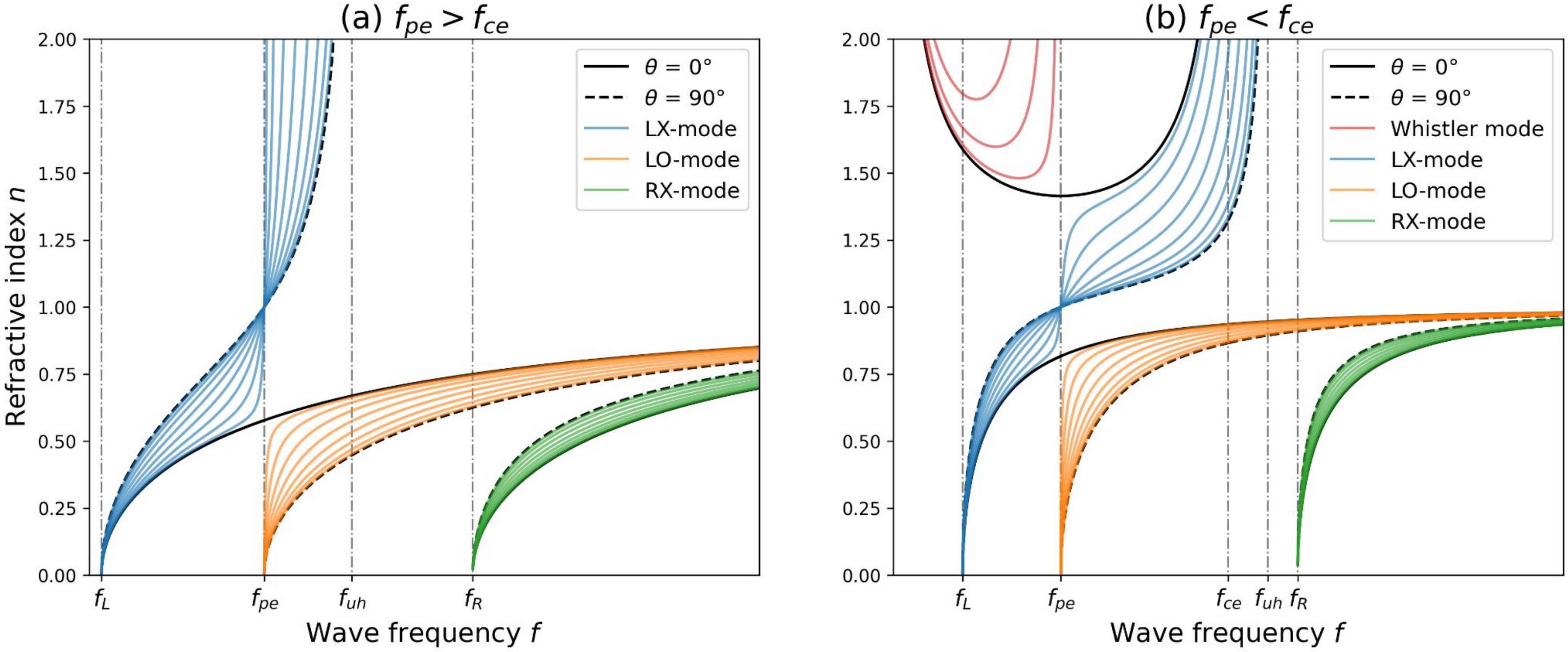

Discussion: Beaming along the frequency gradient

- Snell-Descartes: $n_1 \sin\theta_1 = n_2 \sin\theta_2$, meaning that $\theta_2 \overset{n_2 \gg n_1}{\approx} 0$ and $\mathbf{k} \parallel \nabla n$

- **In a cold collisionless magnetized plasma:** $\nabla n_O \propto -\nabla f_{pe}$ and $\nabla n_X \overset{f \gg f_{ce}}{\approx} \nabla n_O \propto -\nabla f_{pe}$

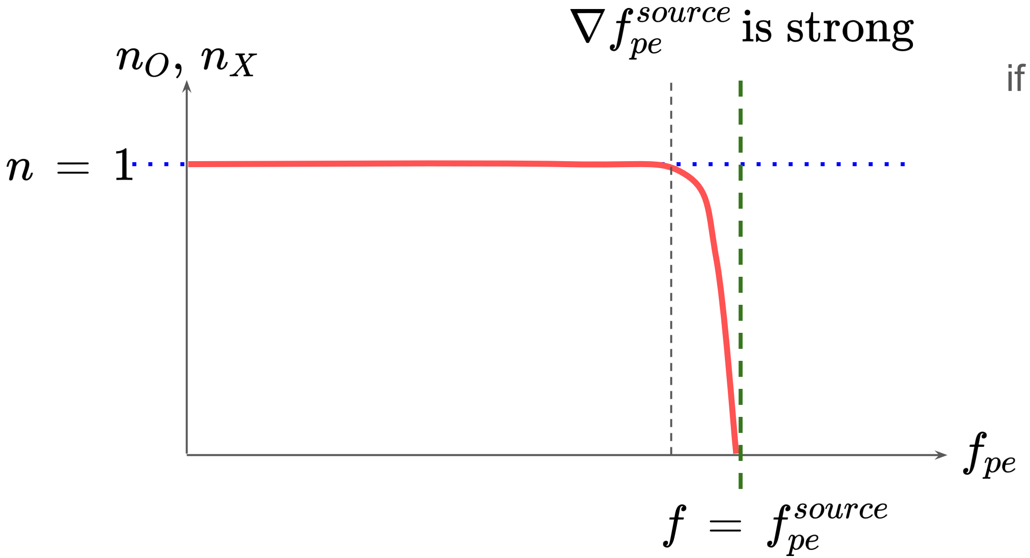

if $|\nabla f_{pe}| \gg 0 \Rightarrow |\nabla n| \gg 0$

- Strong density gradient: $\mathbf{k} \parallel \nabla n \parallel -\nabla f_{pe}$
- The wave **reach quickly n = 1**, meaning that its the **wave is not refracted anymore**
- ***The wave propagation is equivalent to a straight line propagation along the source*** $-\nabla f_{pe}^{source}$

LsPRESSO: Plasma modeling

Imai's (2016) diffusive density model

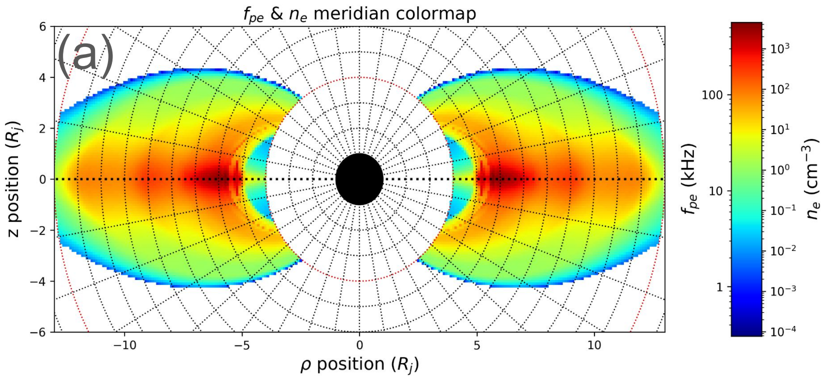

cylindrical symmetry (around z) in the **jovicentrifugal** coordinate system

VIP4 magnetic-field and current-sheath model (Connerney et al. 1998)

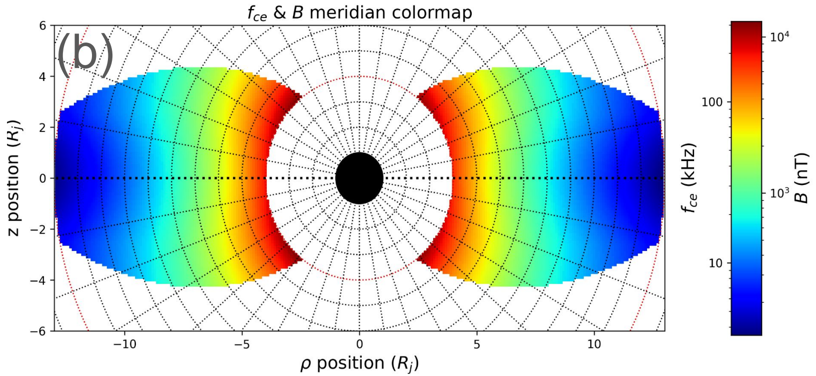

approx cylindrical symmetry (around z) in the **jovimagnetic** coordinate system

Modeled meridian maps of (a) the cold electron density (Imai 2016) and (b) the magnetic-field value (Connerney et al. 1998). The meridian plane here is where the jovicentric, jovicentrifugal and jovimagnetic equators are aligned.

LsPRESSO: Generation Parameters

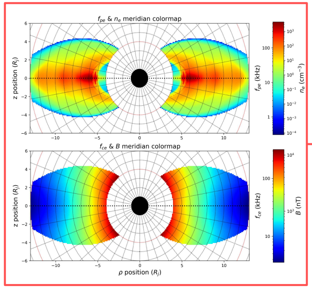

Modeled plasma characteristics (frequencies, cutoffs, gradients)

$$\alpha = angle(\mathbf{B}, \nabla n_e)$$

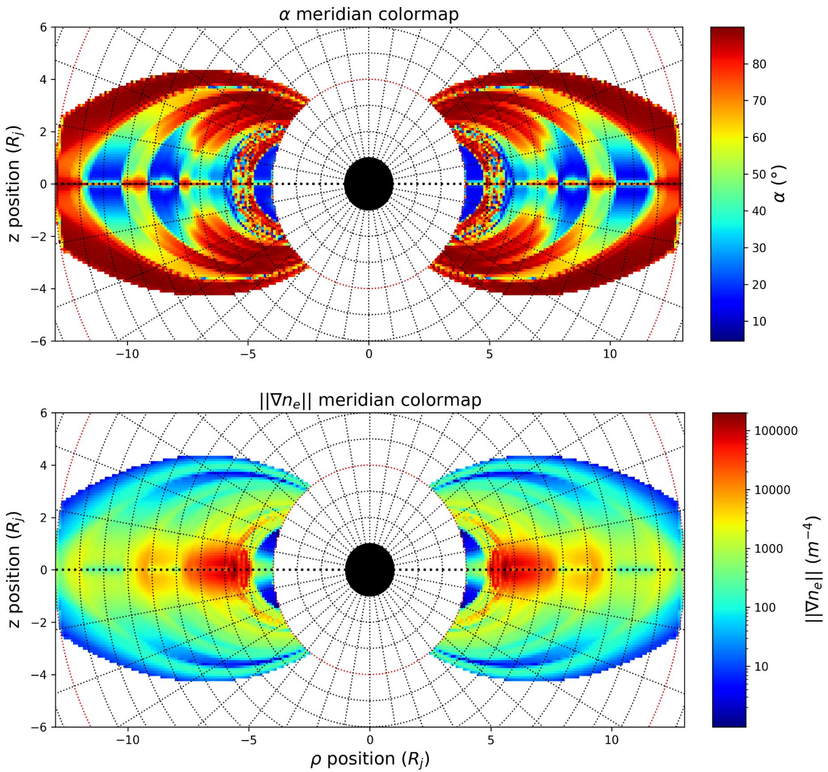

Computed plasma meridian maps of (a) the angle between the density gradient and the magnetic-field and (b) the density gradient strength (Connerney et al. 1998). The meridian plane here is where the jovicentric, jovicentrifugal and jovimagnetic equators are aligned.

Density gradient strength

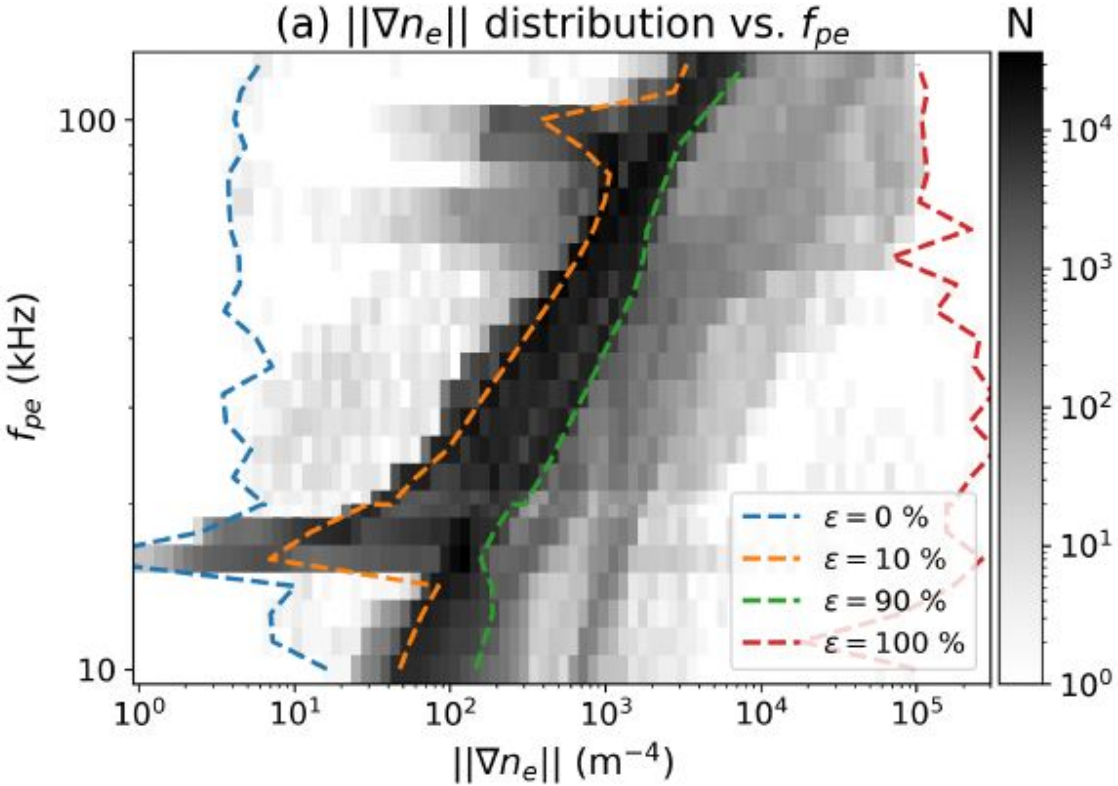

Scenario #3 Parametric Study Results

O-mode

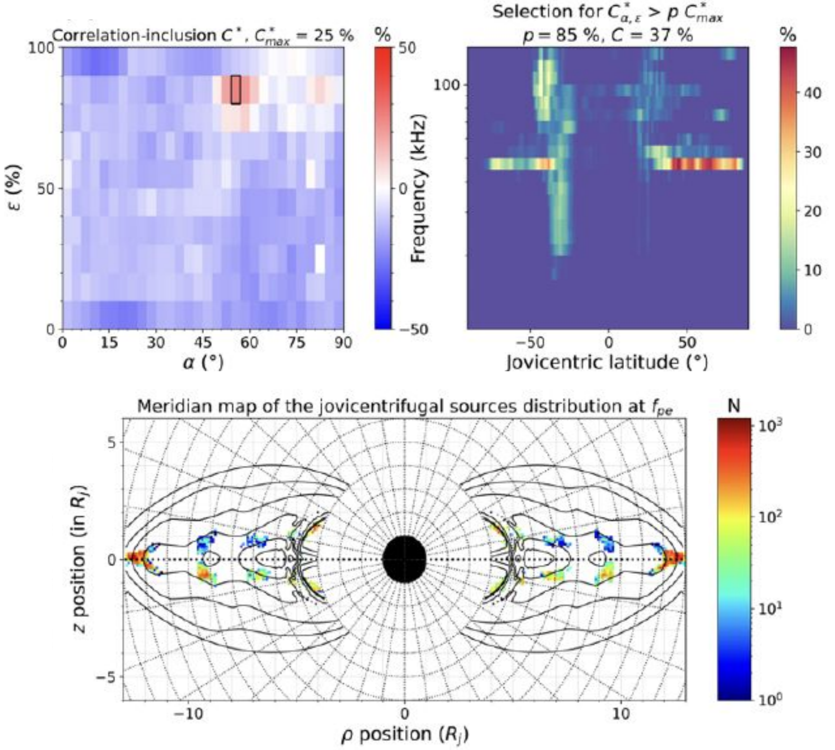

X-mode

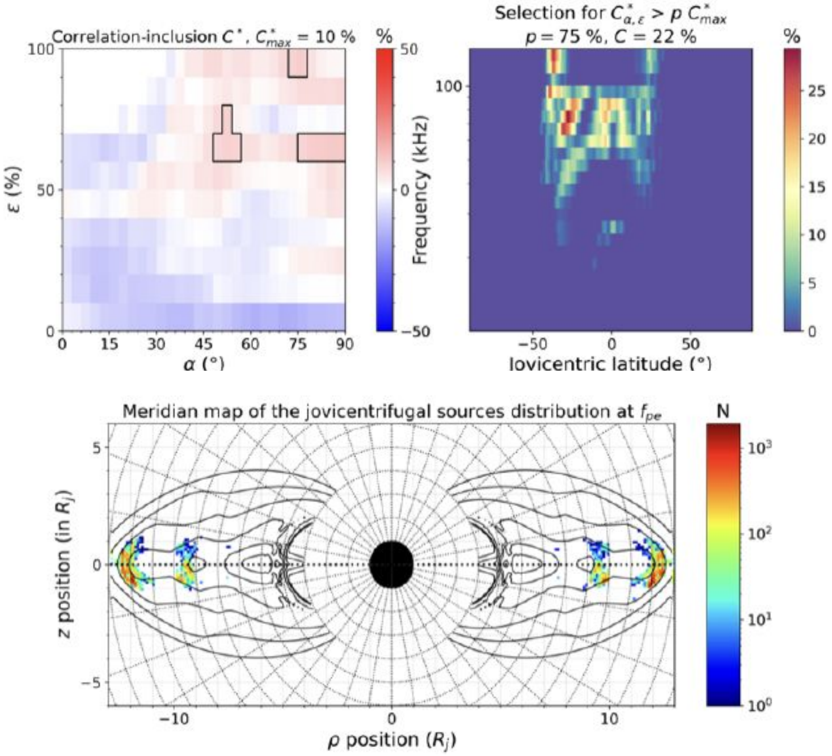

O-mode

X-mode

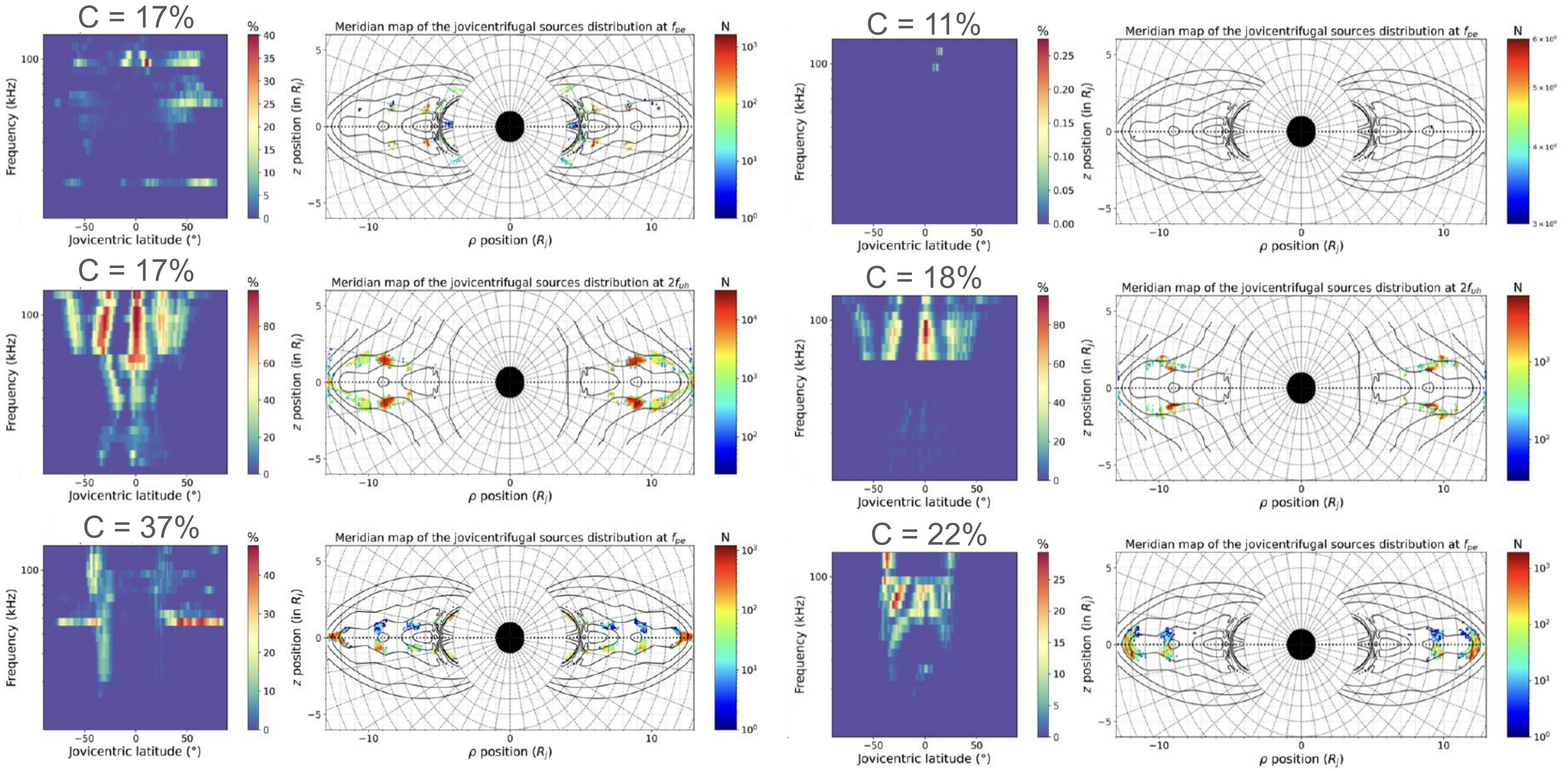

C = 17%
C = 17%
C = 37%
C = 11%
C = 18%
C = 22%
Frequency (kHz)
Jovicentric latitude (°)
%
N
Meridian map of the jovicentrifugal sources distribution at f_{pe}
Meridian map of the jovicentrifugal sources distribution at $2f_{uh}$
z position (in R_j)
ρ position (R_j)

O-mode

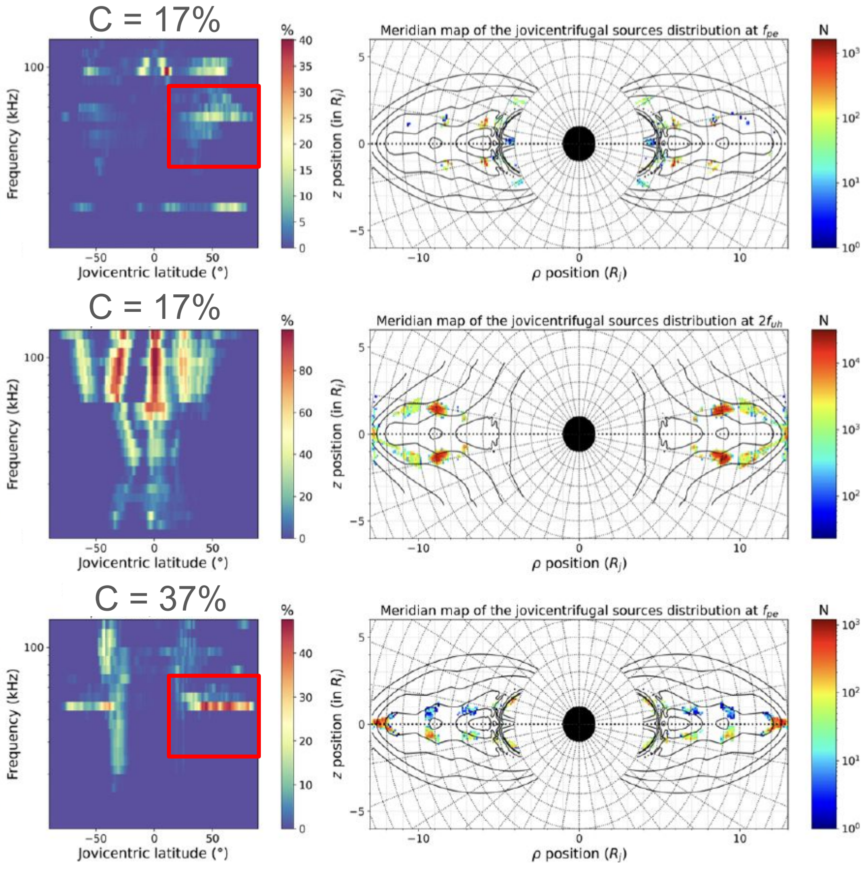

C = 17%
C = 17%
C = 37%
Frequency (kHz)
Jovicentric latitude (°)
%
Meridian map of the jovicentrifugal sources distribution at f_{pe}
Meridian map of the jovicentrifugal sources distribution at $2f_{uh}$
Meridian map of the jovicentrifugal sources distribution at f_{pe}
z position (in R_J)
ρ position (R_J)
N

X-mode

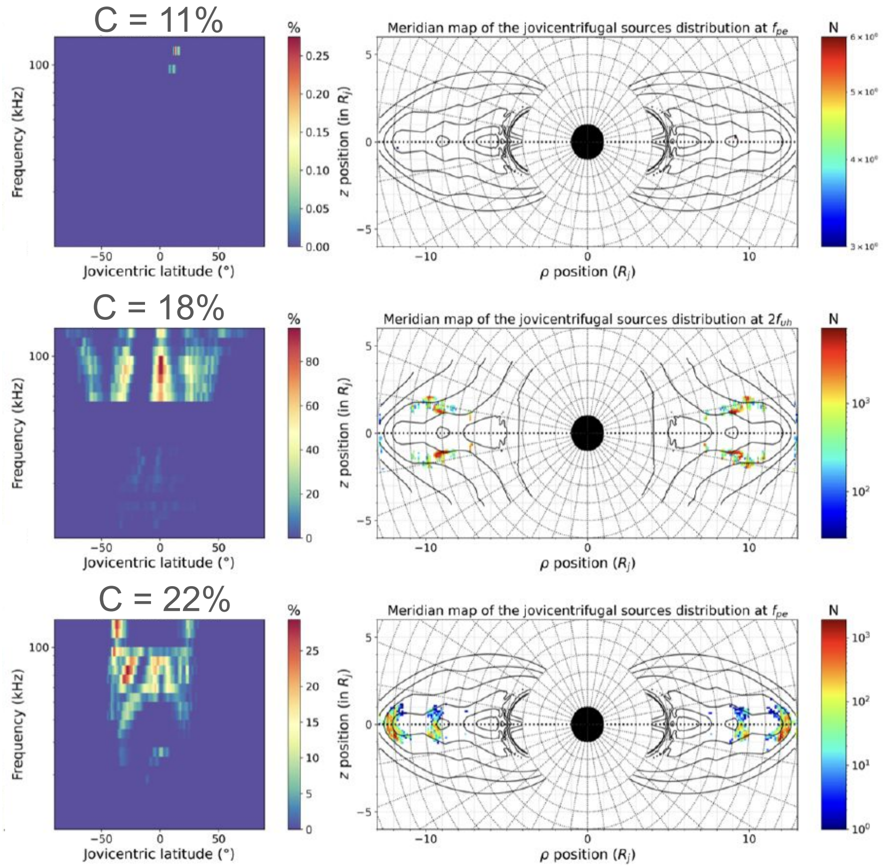

C = 11%
C = 18%
C = 22%
Frequency (kHz)
Jovicentric latitude (°)
%
Meridian map of the jovicentrifugal sources distribution at f_{pe}
Meridian map of the jovicentrifugal sources distribution at $2f_{uh}$
Meridian map of the jovicentrifugal sources distribution at f_{pe}
z position (in R_J)
ρ position (R_J)
N

LsPRESSO: Emission Simulation

Simulation parameters:

- $\alpha = \alpha_A$
- $\epsilon = \epsilon_A$

(α_A, ϵ_A)

Active Source
(= 1 voxel)

(α_I, ϵ_I)

Inactive Source
(= 1 voxel)

(α_I, ϵ_I)

Inactive Source
(= 1 voxel)

LsPRESSO: Emission Simulation

Simulation parameters:

- $\alpha = \alpha_A$
- $\epsilon = \epsilon_A$

Scenario:

- frequency = **f**
- beaming = $\vec{\mathbf{k}}$

Active Source
(= 1 voxel)
frequency at **f**

LsPRESSO: Emission Simulation

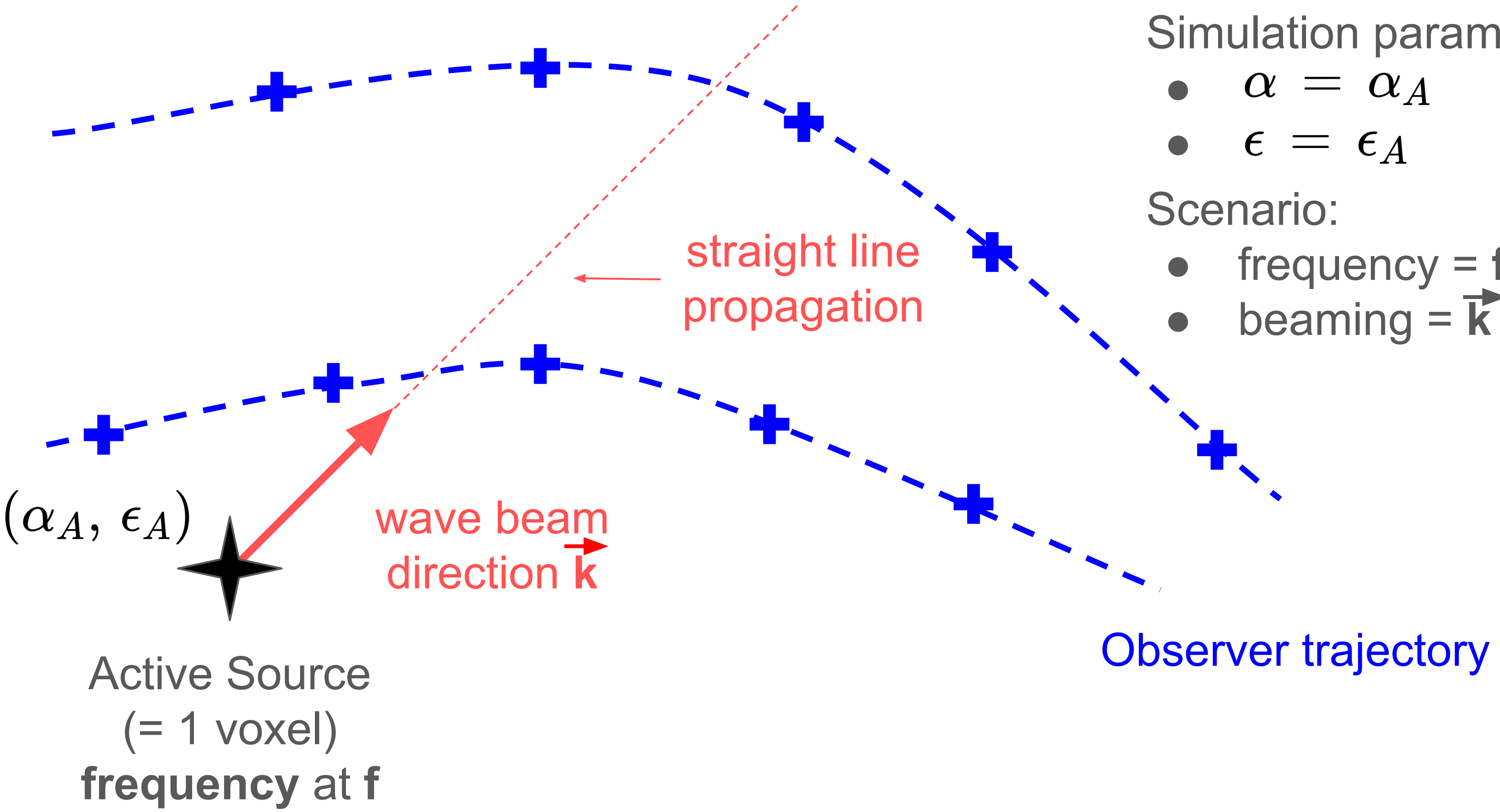

Simulation parameters:

- $\alpha = \alpha_A$
- $\epsilon = \epsilon_A$

Scenario:

- frequency = **f**
- beaming = $\vec{\mathbf{k}}$

LsPRESSO: Emission Simulation

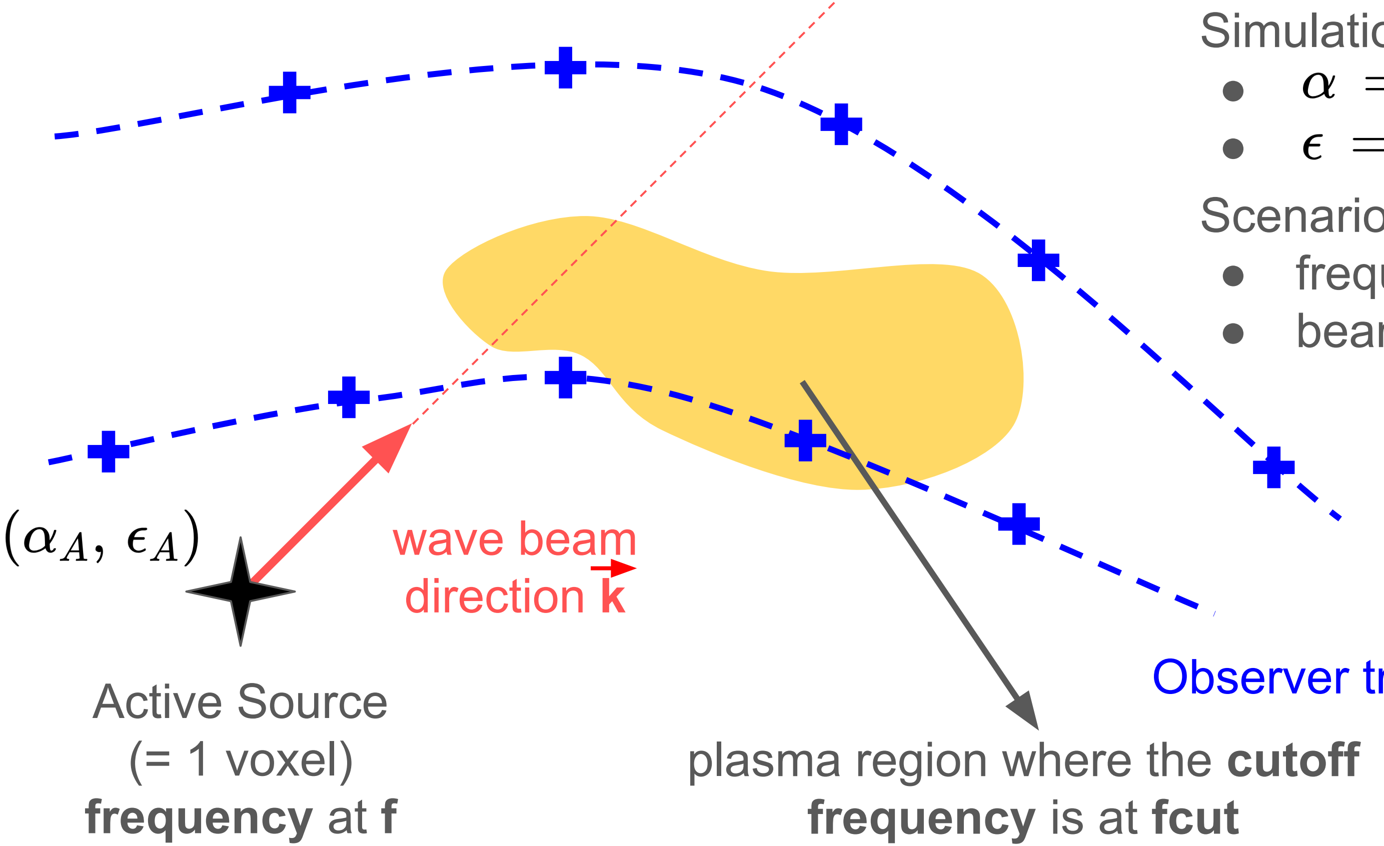

Simulation parameters:

- $\alpha = \alpha_A$
- $\epsilon = \epsilon_A$

Scenario:

- frequency = **f**
- beaming = $\vec{\mathbf{k}}$

LsPRESSO: Emission Simulation

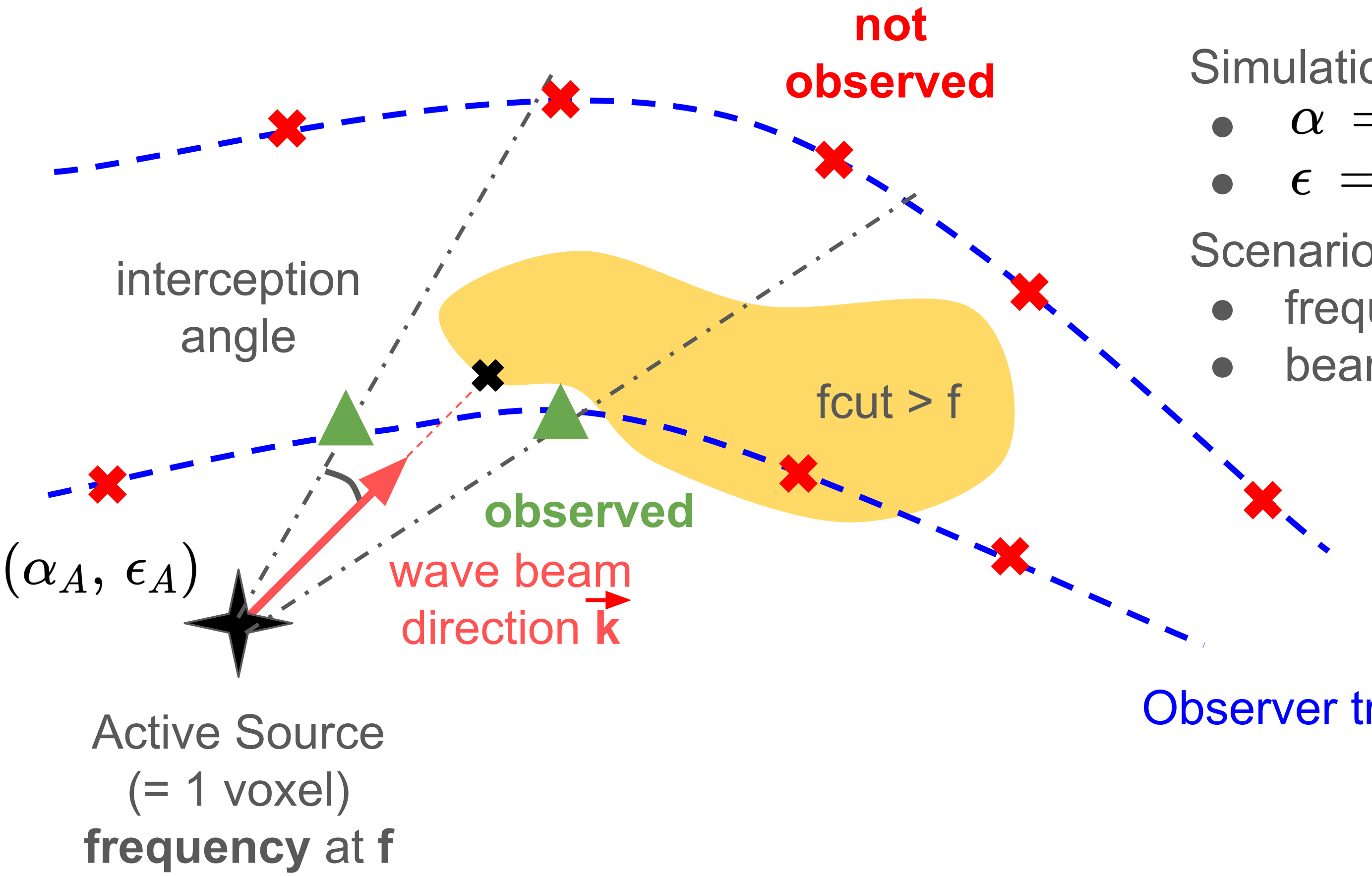

Simulation parameters:

- $\alpha = \alpha_A$
- $\epsilon = \epsilon_A$

Scenario:

- frequency = **f**
- beaming = $\vec{\mathbf{k}}$

Parametric Study

- **We correlate** the modeled distributions to the nKOM distribution as a function of **2 parameters** :
  - $\alpha = angle(\mathbf{B}, \nabla n_e)$
  - $\epsilon = percentile(\|\nabla n_e\|/n_e)$

strongest gradients

weakest gradients

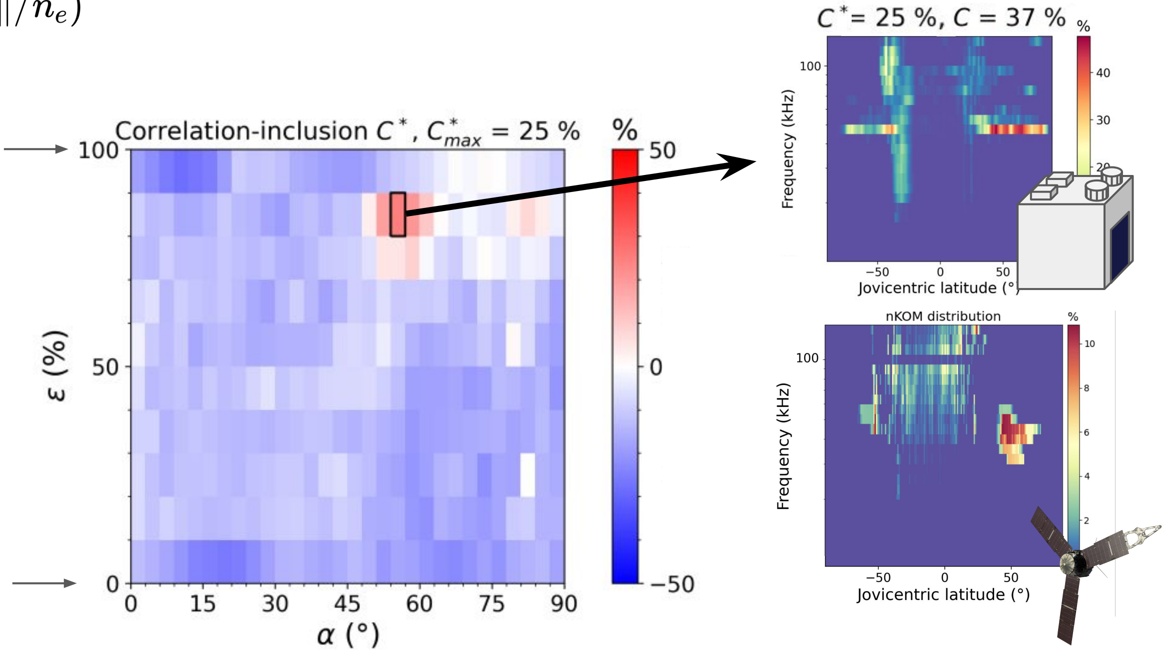

Parametric study: Distributions Combination

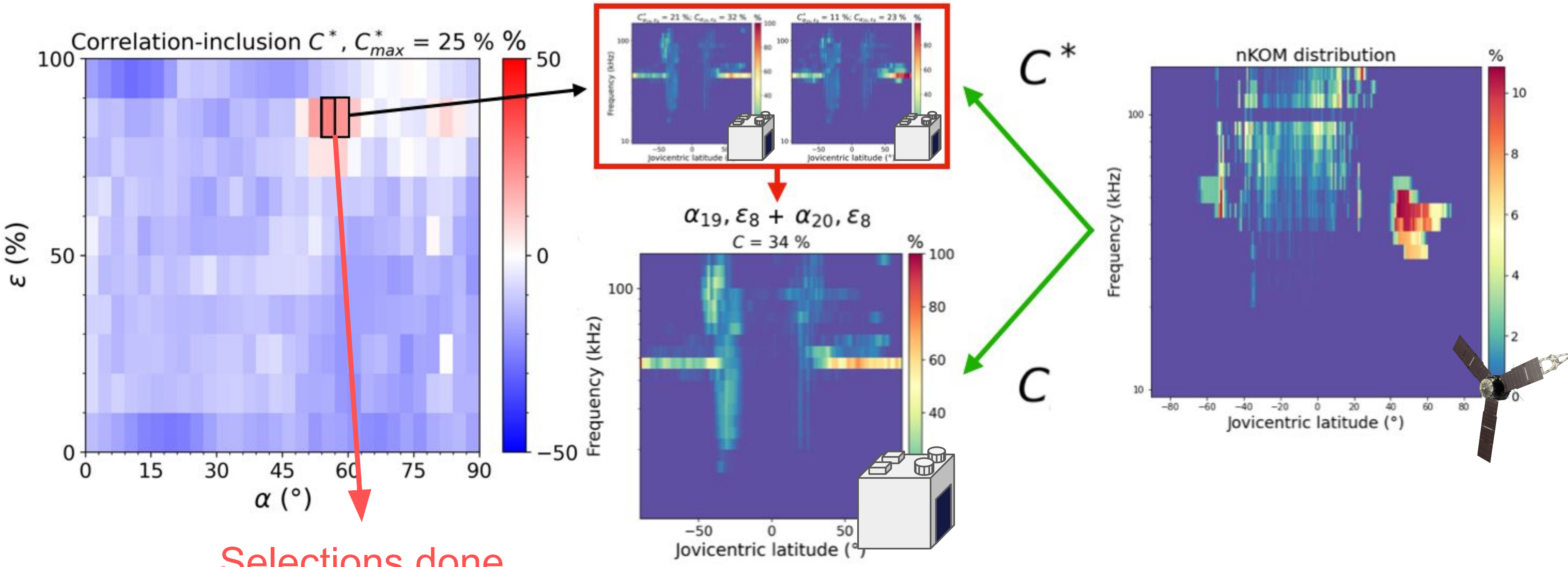

Selections done considering a threshold p in % of max(C*)

here p = 75% of max(C*)

Results: Linear Correlation evolution

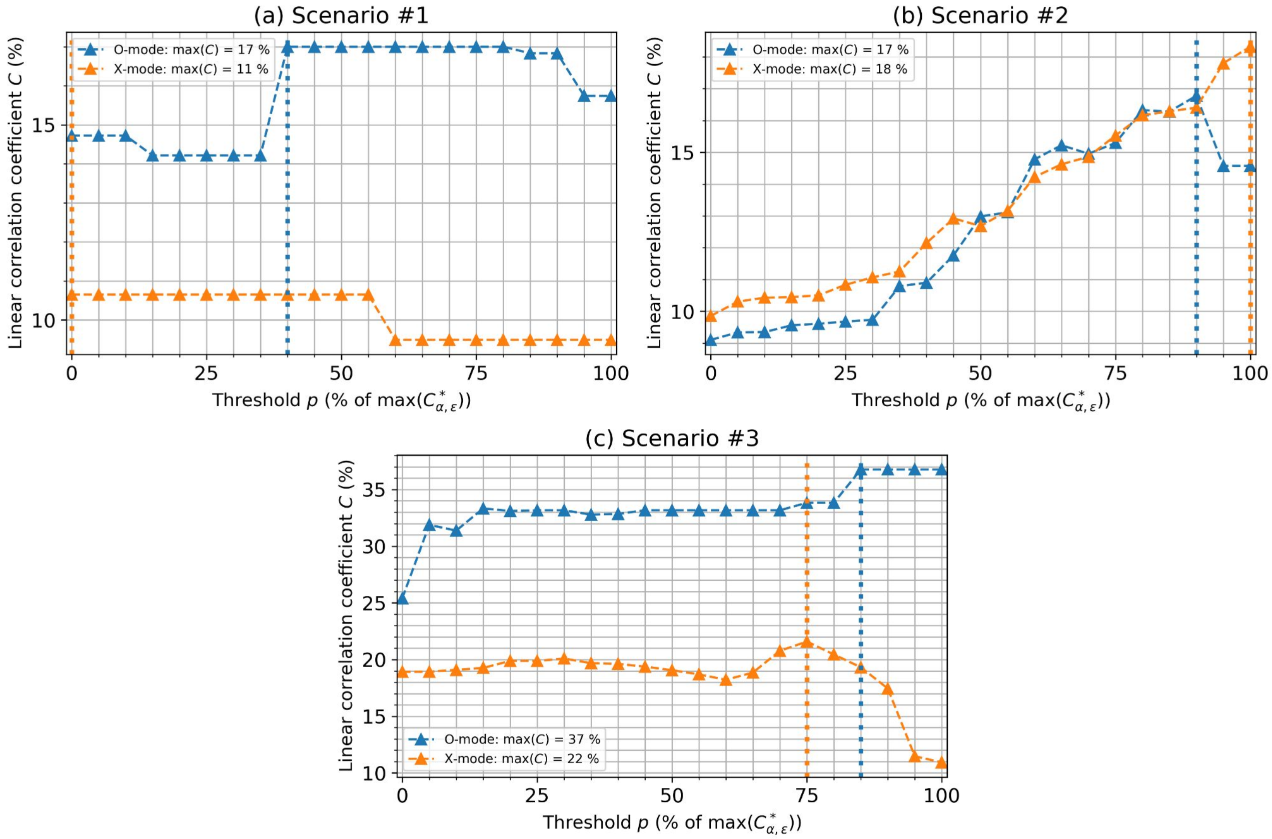

Pearson correlation coefficient evolution as a function of the threshold *p* (in % of max(C*)). Panels (a), (b), (c) and (d) correspond respectively to the scenarios #1, #2, #3 and #4.

Scenario : Reference	Beaming	Scheme
#1 : Jones (1980, 1986, 1987)	$\beta = (\mathbf{k}_+, \mathbf{B})$ $\pi - \beta = (\mathbf{k}_-, \mathbf{B})$	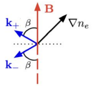
#2 : Fung and Papadopoulos (1987)	$\mathbf{k} \perp \mathbf{B}$	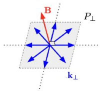
#3 : This study	$\mathbf{k} \parallel - \nabla f_{pe}$	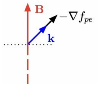

Results: Linear Correlation evolution

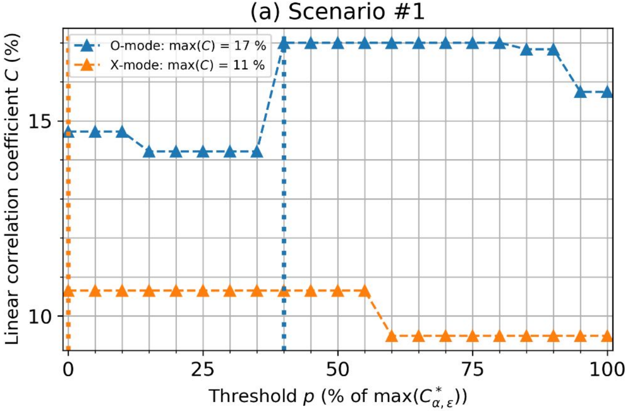

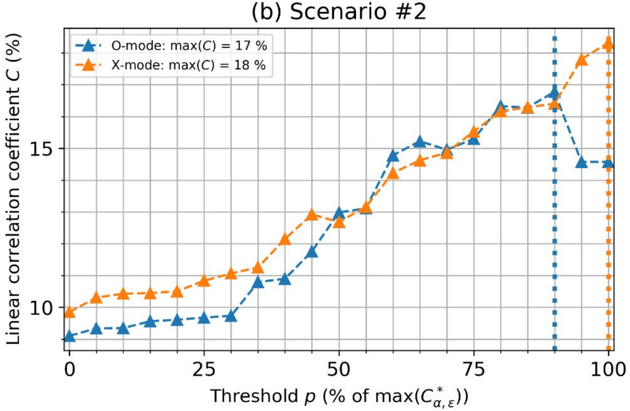

Pearson correlation coefficient evolution as a function of the threshold p (in % of max(C*)). Panels (a), (b), (c) and (d) correspond respectively to the scenarios #1, #2, #3 and #4.

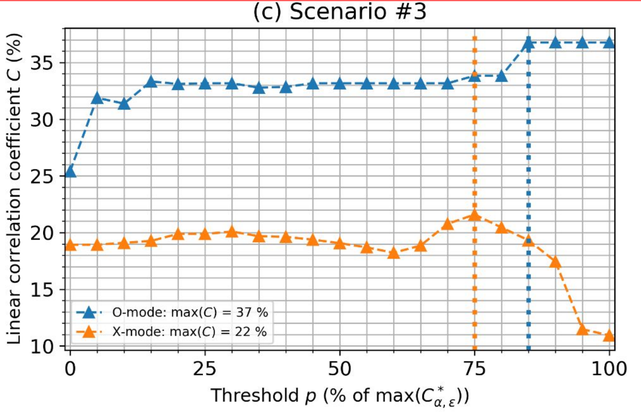

Scenario : Reference	Beaming	Scheme
#1 : Jones (1980, 1986, 1987)	$\beta = (\mathbf{k}_+, \mathbf{B})$ $\pi - \beta = (\mathbf{k}_-, \mathbf{B})$	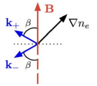
#2 : Fung and Papadopoulos (1987)	$\mathbf{k} \perp \mathbf{B}$	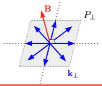
#3 : This study	$\mathbf{k} \parallel - \nabla f_{pe}$	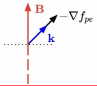

Correlation-Inclusion Coefficient